RAA 2020 Vol. **20** No. **9**, 135(24pp) doi: 10.1088/1674–4527/20/9/135

http://www.raa-journal.org *http://iopscience.iop.org/raa*

Research in Astronomy and Astrophysics

INVITED REVIEWS

The formation of neutron star systems through accretion-induced collapse in white-dwarf binaries

Bo Wang and Dongdong Liu

Yunnan Observatories, Chinese Academy of Sciences, Kunming 650216, China; *wangbo@ynao.ac.cn*
Key Laboratory for the Structure and Evolution of Celestial Objects, Chinese Academy of Sciences, Kunming 650216, China
Center for Astronomical Mega-Science, Chinese Academy of Sciences, Beijing 100101, China
University of Chinese Academy of Sciences, Beijing 100049, China

Received 2020 May 6; accepted 2020 July 8

Abstract The accretion-induced collapse (AIC) scenario was proposed 40 years ago as an evolutionary end state of oxygen-neon white dwarfs (ONe WDs), linking them to the formation of neutron star (NS) systems. However, there has been no direct detection of any AIC event so far, even though there exists a lot of indirect observational evidence. Meanwhile, the evolutionary pathways resulting in NS formation through AIC are still not thoroughly investigated. In this article, we review recent studies on the two classic progenitor models of AIC events, i.e., the single-degenerate model (including the ONe WD+MS/RG/He star channels and the CO WD+He star channel) and the double-degenerate model (including the double CO WD channel, the double ONe WD channel and the ONe WD+CO WD channel). Recent progress on these progenitor models is reviewed, including the evolutionary scenarios leading to AIC events, the initial parameter space for producing AIC events and the related objects (e.g., the pre-AIC systems and the post-AIC systems). For the single-degenerate model, the pre-AIC systems (i.e., the progenitor systems of AIC events) could potentially be identified as supersoft X-ray sources, symbiotics and cataclysmic variables (such as classical novae, recurrent novae, Ne novae and He novae) in the observations, whereas the post-AIC systems (i.e., NS systems) could potentially be identified as low-/intermediate-mass X-ray binaries, and the resulting low-/intermediate-mass binary pulsars, most notably millisecond pulsars. For the double-degenerate model, the pre-AIC systems are close double WDs with short orbital periods, whereas the post-AIC systems are single isolated NSs that may correspond to a specific kind of NS with peculiar properties. We also review the predicted rates of AIC events, the mass distribution of NSs produced via AIC and the gravitational wave (GW) signals from double WDs that are potential GW sources in the Galaxy in the context of future space-based GW detectors, such as LISA, TianQin, Taiji, etc. Recent theoretical and observational constraints on the detection of AIC events are summarized. In order to confirm the existence of the AIC process, and resolve this long-term issue presented by current stellar evolution theories, more numerical simulations and observational identifications are required.

Key words: binaries: close — white dwarfs — supernovae: general — stars: neutron — stars: evolution

1 INTRODUCTION

Compact objects are the product of late stellar evolution, which can be divided into white dwarfs (WDs), neutron stars (NSs) and black holes. WDs are the endpoint of the evolution of low-/intermediate-mass stars, accounting for the final outcome of about 97% of all stars in our Galaxy (e.g., Fontaine et al. 2001; Parsons et al. 2020). According to the underlying compositions, this kind of compact object can be mainly divided into He WDs, carbon-oxygen (CO) WDs and oxygen-neon (ONe) WDs (e.g., Paczyński 1970; Han et al. 1994; Eggleton 2006; Camisassa et al. 2019). Note that some transitional hybrid WDs have been predicted by the stellar evolution theories but not confirmed in observations. For example, He-rich WDs (i.e., HeCO WDs, in which a CO-rich core is surrounded by a

He-rich mantle; see Iben & Tutukov 1985), CONe WDs (an unburnt CO core surrounded by a thick ONe zone; e.g., Denissenkov et al. 2013; Chen et al. 2014), COSi WDs (an unburnt CO core surrounded by a Si-rich shell; see Wu et al. 2020), OSi WDs (see Wu & Wang 2019; Wu et al. 2019), Si WDs (see Schwab et al. 2016), etc.

It has been generally believed that CO WDs in binaries will form type Ia supernovae (SNe Ia) when they grow in mass close to the Chandrasekhar limit ($M_{\rm Ch}$; e.g., Hoyle & Fowler 1960; Nomoto et al. 1984; Podsiadlowski 2010; Wang & Han 2012). However, ONe WDs are predicted to collapse into NSs through electron-capture reactions by Mg and Ne when they increase their mass close to $M_{\rm Ch}$, in which the transformation from ONe WDs to NSs is referred to as the accretion-induced collapse (AIC) process that was proposed 40 years ago based on stellar evolution theories (e.g., Nomoto et al. 1979; Miyaji et al. 1980; Taam & van den Heuvel 1986; Canal et al. 1990a; Nomoto & Kondo 1991; Schwab et al. 2015; Schwab & Rocha 2019). Some recent studies claimed that ONe WDs can experience explosive oxygen or neon burning and finally form a subclass of SNe Ia (e.g., Marquardt et al. 2015; Jones et al. 2016, see also Isern et al. 1991). The final outcome of ONe WDs (collapse or explosion) is mainly determined by the competition between electron-capture reactions and nuclear burning. By simulating the long-term evolution of mass-accreting ONe WDs with different initial masses and various mass-accretion rates, Wu & Wang (2018) found that the central temperature of ONe WDs cannot reach the temperature for explosive oxygen or neon burning as the neutrino-loss apparently increases with the central temperature. Thus, the final outcome of ONe WDs with $M_{\rm Ch}$ is to collapse into NSs.

NSs have been generally thought to be produced through core-collapse supernovae (SNe) and electron-capture SNe (e.g., van den Heuvel 2009). As a kind of electron-capture SNe, AIC events are expected to be relatively faint optical transients (e.g., Woosley & Baron 1992). A small amount ($\sim 10^{-3} - 10^{-1}\,M_{\odot}$) of the ejecta mass is predicted during the collapse, and the ^{56}Ni synthesized is possibly $\sim 10^{-4} - 10^{-2}\,M_{\odot}$ (e.g., Fryer et al. 1999; Dessart et al. 2006, 2007; Metzger et al. 2009; Darbha et al. 2010). It has been suggested that AIC events are fainter than those of typical normal SNe Ia by 5 mag or more, and last for only a few days to a week (e.g., Piro & Thompson 2014). Thus, they are relatively short-lived and most likely underluminous. This indicates that this kind of object is difficult to be discovered. Piro & Kollmeier (2013) suggested that a transient radio source may appear after the AIC event, which can last for a few months.

Up to now, there has been no reported direct detection for such events, but a lot of indirect evidence exists in observations. The remnants of AIC process are NS systems, which can be utilized to explain a variety of the observed troublesome NS systems that cannot be reproduced by core-collapse SNe (e.g., Canal et al. 1990b; Tauris et al. 2013; Liu & Li 2017; Ablimit 2019), as follows:

(1) It has been suggested that some of observed pulsars in globular clusters are significantly younger than the clusters themselves, which can be explained by the AIC scenario that could produce newborn NSs with small kicks (e.g., Boyles et al. 2011).
(2) The AIC scenario provides an alternative way to explain the formation of some millisecond pulsars (MSPs; e.g., Bhattacharya & van den Heuvel 1991; Ivanova et al. 2008; Hurley et al. 2010; Freire & Tauris 2014). Hurley et al. (2010) found that the rates of binary MSPs from the AIC scenario are comparable to those from core-collapse SNe. This indicates that the AIC scenario plays a key role in the production of binary MSPs. Note that Chen et al. (2011a) argued that the AIC scenario cannot form eccentric binary MSPs with an orbital period of $\gtrsim 20\,{\rm d}$ even though a high kick is considered. This is because the formation of eccentric binary MSPs needs a high kick during the AIC, but the high kick is more likely to disrupt the binary when the orbit is too wide, finally forming more isolated MSPs (see Chen et al. 2011a).
(3) The AIC scenario can be employed to explain a large fraction of NSs in globular clusters and the formation of recycled pulsars with observed low space velocities due to the small kicks and the small amount of mass-loss during collapse (e.g., Bailyn & Grindlay 1990; Kitaura et al. 2006; Dessart et al. 2006).
(4) The recycling process of the AIC scenario can be applied to explain some mass-accreting NSs with strong magnetic fields in low-mass X-ray binaries (LMXBs) and some strongly magnetized pulsars with He WD companions, which have undergone extensive mass-transfer but do not have too much matter accumulated onto the surface of the NSs (e.g., Taam & van den Heuvel 1986; van Paradijs et al. 1997; Li & Wang 1998; Xu & Li 2009).
(5) The AIC scenario has been invoked as an alternative mechanism for the formation of low-/intermediate-mass X-ray binaries and low-/intermediate-mass binary pulsars (e.g., van den Heuvel 1984; Canal et al. 1990b; Nomoto & Kondo 1991; Li & Wang 1998; Tauris et al. 2012; Liu et al. 2018a).

Meanwhile, the AIC scenario has been proposed as a promising way to form some important events, as follows: (1) The ejecta from the AIC process has been claimed as a possible source of r-process nucleosynthesis (e.g., Wheeler et al. 1998; Fryer et al. 1999; Qian & Wasserburg 2007). (2) The AIC process has been proposed as a source of gravitational wave (GW) emission (e.g., Abdikamalov et al. 2010). (3) The AIC scenario may be a novel source of cosmic rays and of cosmological gamma-ray bursts (e.g., Usov 1992; Dar et al. 1992; Lyutikov & Toonen 2017). Piro & Kollmeier (2016) recently argued that the AIC scenario can potentially form rapidly spinning magnetars, in which the newborn magnetars supply an attractive site for producing ultrahigh-energy cosmic rays. (4) It has been suggested that AIC may provide an alternative way to result in fast radio bursts (e.g., Moriya 2016; Cao et al. 2018; Margalit et al. 2019). (5) Belczyński et al. (2018) recently argued that the AIC scenario can contribute to the formation of double NSs in the globular cluster dynamical channel. In this channel, an NS+ONe WD binary interacts with a CO WD, during which the ONe WD merges with the CO WD, leading to the formation of an NS via AIC (see fig. 3 of Belczyński et al. 2018).

Despite the potential importance of the AIC process, it is still uncertain about their progenitor models. Meanwhile, the theoretical rates of AIC events remain highly uncertain. Similar to the progenitor models of SNe Ia, two classic kinds of progenitor models for AIC events have been proposed so far (i.e., the single-degenerate model and the double-degenerate model), as follows:

(1) *The single-degenerate model*. In this model, an ONe WD grows in mass by accreting matter from its non-degenerate companion. An AIC event may be produced once the ONe WD increases its mass close to $M_{\rm Ch}$ (e.g., Nomoto & Kondo 1991; Yungelson & Livio 1998; Ivanova & Taam 2004; Tauris et al. 2013; Brooks et al. 2017; Liu et al. 2018a; Wang 2018a; Ruiter et al. 2019). The single-degenerate model mainly produces NS binary systems through AIC.

(2) *The double-degenerate model*. This model is usually called merger-induced collapse, in which an AIC event results from the merging of double WDs with a total mass heavier than $M_{\rm Ch}$; the merging of double WDs was caused by GW radiation that results in its orbit shrinking (e.g., Nomoto & Iben 1985; Saio & Nomoto 1985; Ruiter et al. 2019; Liu & Wang 2020). In addition to the orbital evolution caused by GW radiation, the merger of double WDs in triple systems can be caused by the Kozai-Lidov mechanism, in which secular gravitational effects result in eccentricity oscillations in the inner binary (see Kozai 1962; Lidov 1962). For a recent review on the Kozai-Lidov mechanism, see Naoz (2016). The merger-induced collapse for double-degenerate binaries mainly produces single isolated NSs, whereas the outcomes of triple systems via AIC likely form NS binaries with long orbital periods.

In this article, we mainly review recent progress on the currently most popular progenitor models of AIC events, including the single-degenerate model in Section 2 and the double-degenerate model in Section 3. In Section 4, we review recent results of binary population synthesis for producing AIC events, including the predicted rates of AIC events in the Galaxy, the mass distribution of NSs via AIC and the GW signals from double WDs that may produce AIC events. We summarize recent theoretical and observational constraints on the detection of AIC events in Section 5. Finally, a summary is given in Section 6.

2 THE SINGLE-DEGENERATE MODEL

In this model, an ONe WD grows in mass by accreting H-/He-rich matter from its non-degenerate companion that could be a main sequence (MS) or a slightly evolved star (the ONe WD+MS channel), a red giant (RG) star (the ONe WD+RG channel) or even a He star (the ONe WD+He star channel). The accreted matter will be burned into C and O, and accumulate on the surface of the ONe WD, resulting in mass increase of the WD. When the ONe WD increases its mass close to $M_{\rm Ch}$, an AIC event may be produced. Note that the maximum stable mass for a WD is likely to be larger than $M_{\rm Ch}$ in consideration of rotation (e.g., Ostriker & Bodenheimer 1968; Yoon & Langer 2004; Wang et al. 2014).

Tauris et al. (2013) studied the binary computations of ONe WD+MS/RG/He star systems that may undergo the AIC process and then be recycled to produce binary pulsars. However, they only considered the case with the initial mass of ONe WD $M^{\rm i}_{\rm ONe} = 1.2\,M_{\odot}$. By adopting the optically thick wind assumption (see Hachisu et al. 1996), Wang (2018a) investigated the ONe WD+MS/RG/He star channels for producing AIC events in a systematic way with different $M^{\rm i}_{\rm ONe}$. Compared with the results of Tauris et al. (2013), the initial regions of AIC events obtained by Wang (2018a) are notably enlarged, mainly due to different prescriptions for the case of rapid mass-transfer process. In addition, Wang et al. (2017) recently found that the CO WD+He star systems may also form NS systems through the AIC process when off-center carbon ignition happens on the surface of the CO WD, known as the CO WD+He star channel (see also Brooks et al. 2016).

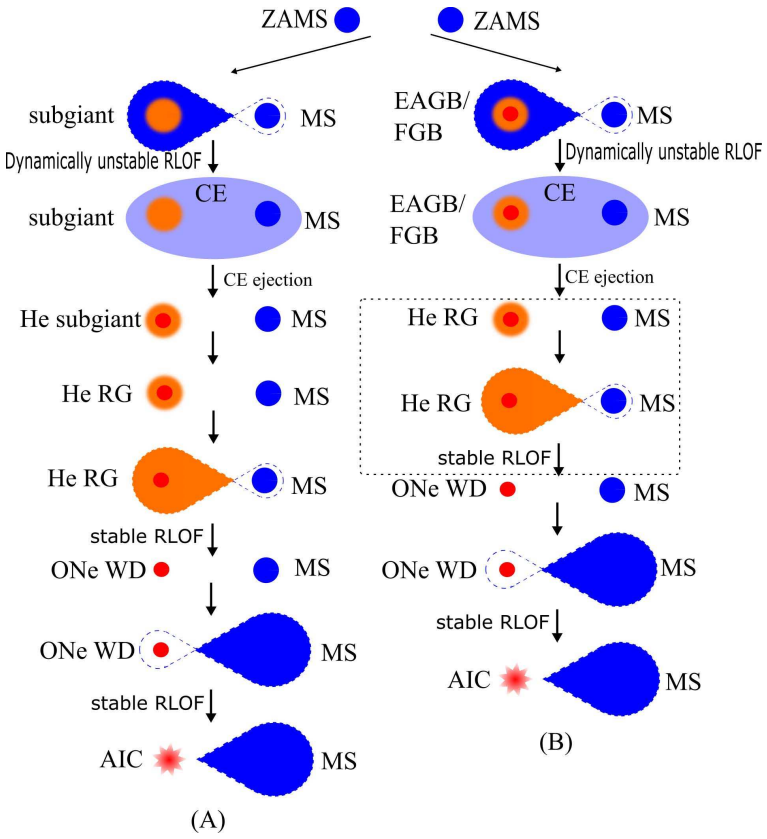

Fig. 1 Evolutionary scenarios to ONe WD+MS systems that can form AIC events. In Scenario B, some cases will not experience the second RLOF (*dashed box*).

2.1 The ONe WD+MS Channel

2.1.1 Evolutionary scenarios

In this channel, AIC events originate from the evolution of ONe WD+MS systems. According to the evolutionary stage of the primordial primary (massive star) when it first fills its Roche lobe, there are two evolutionary scenarios to form ONe WD+MS systems and then produce AIC events (see Fig. 1), in which Scenario A is the main way to form AIC events (see Wang 2018a).

Scenario A: The primordial primary fills its Roche lobe at the Hertzsprung gap (HG) stage, leading to a case B mass-transfer process. In this case, a common envelope (CE) may be formed because of the large mass-ratio or the convective envelope of the Roche lobe filled star. After ejection of CE, the primordial primary turns out to be a He subgiant star. The primary continues to evolve and will form a He RG star when its central He is exhausted. The primary will expand quickly at this stage and will fill its Roche lobe again, resulting in a stable mass-transfer process. After that, the primary becomes an ONe WD, forming an ONe WD+MS system. For this scenario, the initial parameters of the primordial binaries for producing AIC events are in the range of $M_{1,\rm i} \sim 8-11\,M_\odot$, $q = M_{2,\rm i}/M_{1,\rm i} \sim 0.2-0.4$ and $P^{\rm i} \sim 40-900$ d, in which $M_{1,\rm i}$, $M_{2,\rm i}$, q and $P^{\rm i}$ are the initial masses of the primordial primary and the secondary, the initial mass-ratio and the initial orbital period of the primordial systems, respectively[1]. About three quarters of AIC events from the ONe SNe Ia channel are produced through this scenario.

Scenario B: The primordial primary first fills its Roche lobe at the early asymptotic giant branch (EAGB) stage or the first giant branch (FGB) stage, and then a CE may be formed due to the dynamically unstable mass-transfer. If the CE can be ejected, the primary will turn into a He RG star. The He RG continues to evolve and will quickly fill its Roche lobe again, leading to a stable Roche lobe overflow (RLOF) process. After the mass-transfer process, the primary becomes an ONe WD, resulting in the formation of an ONe SNe Ia system. For this sce-

[1] The range of initial parameters was obtained under some specific assumptions for both the primordial binaries and binary interactions in the binary population synthesis studies (see Wang 2018a; Liu & Wang 2020). Here, we set the CE ejection parameter $\alpha_{\rm CE}\lambda$ to be 1.5. If we adopt a low value of $\alpha_{\rm CE}\lambda$ (e.g., 0.5), the initial orbital period will become longer as the primordial binaries could release more orbital energy during the CE ejection so that they can evolve to the initial parameter regions for producing AIC events.

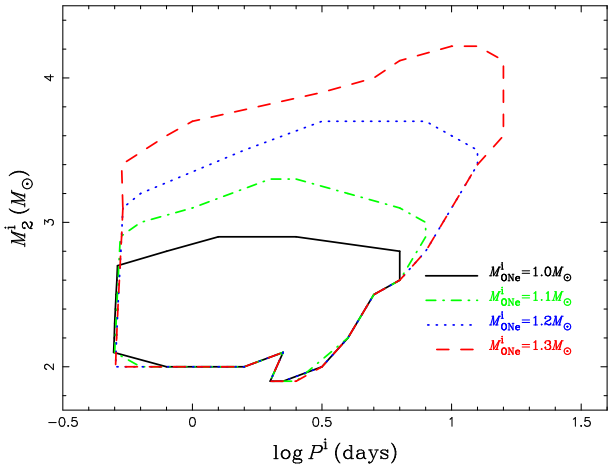

Fig. 2 Initial parameter regions of ONe WD+MS systems for producing AIC events in the $\log P^{\rm i} - M_2^{\rm i}$ plane with various $M_{\rm ONe}^{\rm i}$. Source: From Wang (2018a).

nario, the initial parameters of the primordial binaries for producing AIC events are in the range of $M_{1,\rm i} \sim 6-8\,M_\odot$, $q \sim 0.2-0.4$ and $P^{\rm i} \sim 400-1000\,{\rm d}$. About one quarter of AIC events from the ONe SNe Ia channel are produced through this scenario. Note that the mass-transfer process from a He RG to an MS indicated by the dashed box of Figure 1 may not be indispensable in some cases.

2.1.2 *Parameter space for AIC events*

After the formation of ONe WD+MS systems, the ONe WD could accrete H-rich matter from its MS companion when it fills its Roche lobe. The accreted H-rich matter is burned into He, and then the He is processed into C and O. The ONe WD may collapse into an NS when it grows in mass close to $M_{\rm Ch}$. Figure 2 shows the initial parameter regions of AIC events for the ONe WD+MS channel in the $\log P^{\rm i} - M_2^{\rm i}$ plane with different $M_{\rm ONe}^{\rm i}$, where $M_2^{\rm i}$ is the initial mass of the MS star and $P^{\rm i}$ is the initial orbital period of the ONe WD+MS system. In order to produce AIC events, the ONe WD should have MS companions with initial masses of $\sim 2-4.2\,M_\odot$ and initial orbital periods of $\sim 0.5-16\,{\rm d}$.

The boundaries of the initial regions in Figure 2 are mainly constrained by the following conditions: (1) The lower boundaries are set by a low mass-transfer rate that prevents the ONe WDs growing in mass to $M_{\rm Ch}$ during H-shell flashes. (2) The upper boundaries are constrained by a high mass-transfer rate owing to a large mass-ratio between the MS star and the ONe WD, making the binaries lose too much mass through optically thick wind. (3) Binaries beyond the right boundaries undergo a relatively rapid mass-transfer process due to rapid expansion of the MS donors during the HG stage, losing too much mass via optically thick wind. (4) The left boundaries are determined by the case that RLOF starts when the MS donor is still in the zero age stage.

In addition, metallicities may have an important effect on the initial contours for producing AIC events. In Figure 2, we set metallicitity $Z = 0.02$ (also in Fig. 4 and Figs. 6–7). If a different metallicity is adopted, the initial contours in Figure 2 will be changed. The initial contours for producing WDs with $M_{\rm Ch}$ would be enlarged to have larger mass donors and longer orbital periods with the increase in metallicity (e.g., Meng et al. 2009; Wang & Han 2010). The influence of metallicity on the initial contours in Figure 4 and Figures 6–7 is similar to that of Figure 2. For more studies on the WD+MS channel for producing WDs with $M_{\rm Ch}$, see, e.g., Li & van den Heuvel (1997), Hachisu et al. (1999a), Langer et al. (2000), Han & Podsiadlowski (2004, 2006), Wang et al. (2010), etc.

2.1.3 *Pre-AIC systems*

In the observations, the pre-AIC systems (i.e., the progenitor systems of AIC events) with MS donors could potentially be identified as supersoft X-ray sources and cataclysmic variables (e.g., classical novae, recurrent novae and Ne novae) during the mass-accretion process. Supersoft X-ray sources are CO/ONe WD binaries where steady nuclear burning (stable H-/He-shell burning) occurs on the surface of the WDs (e.g., van den Heuvel et al. 1992; Rappaport et al. 1994), which are strong progenitor candidates of AIC events if the ONe WD can grow in mass close to $M_{\rm Ch}$.

Classical novae and recurrent novae are thermonuclear explosions that happen in the surface shell of accreting CO/ONe WDs (i.e., CO WDs or ONe WDs) in binaries, eventually resulting in the dynamic ejection of the surface shell. They usually contain a massive WD with mass-accretion rates below the minimum rate for stable shell nuclear burning (see Warner 1995). Wu et al. (2017) recently found that nova outbursts can make the WDs grow in mass to $M_{\rm Ch}$. U Sco is a recurrent nova, which contains a $1.55 \pm 0.24\,M_\odot$ WD and a $0.88 \pm 0.17\,M_\odot$ MS donor with an orbital period of $\sim 0.163\,{\rm d}$ (e.g., Hachisu et al. 2000; Thoroughgood et al. 2001). Mason (2011) derived a relatively high [Ne/O] abundance for U Sco during its outburst in 2010, indicating that it may be a nova outburst which occurred on the surface of an ONe WD. However, Mason (2011) neglected the effects of collisions on the formation of an emission line spectrum (see also Mikołajewska & Shara 2017). Mason (2013) corrected this computational error and suggested only a mild overabun-

dance of Ne in the ejecta of U Sco, possibly consistent with a CO WD.

Ne novae are a subclass of classical novae, in which an important feature is the significant enrichment of Ne detected in the ejecta (e.g., Andrea et al. 1994; Gehrz et al. 1998; Denissenkov et al. 2014). There are many Ne novae in the observations, which are thought to occur on the most massive WDs (e.g., Wanajo et al. 1999; Shore et al. 2003, 2013; Downen et al. 2013). It has been estimated that about 1/3 of the observed nova systems contain ONe WDs (see Gil-Pons et al. 2003). Casanova et al. (2016) recently performed 3D simulations of mixing at the core-envelope interface during nova outbursts. They found that ONe WDs (as in Ne novae) produce higher metallicity enhancements in the ejecta than that on the surface of CO WDs (i.e., non-Ne novae; see also Glasner et al. 2012). The ONe WD usually contains an ONe core surrounded by a CO-rich mantle, where extensive He-shell burning has occurred (e.g., Gil-Pons & García-Berro 2001; Gil-Pons et al. 2003).

2.1.4 Post-AIC systems

After the AIC process, the MS donor may fill its Roche lobe again, and transfer H-rich matter and angular momentum onto the surface of the newborn NS. The post-AIC systems with MS donors could potentially be identified as LMXBs and the resulting low-mass binary pulsars (LMBPs) in the observations, especially most notably MSPs. The post-AIC evolution with MS donors is similar to that of normal LMXB evolution. The only difference is that the MS donor has already lost some of its matter during the pre-AIC evolution. Podsiadlowski et al. (2002) suggested that some of the LMXBs consisting of an NS and an MS donor with initial orbital periods below the bifurcation period may eventually evolve to ultra-compact X-ray binaries (UCXBs) that are a subclass of LMXBs with ultra-short orbital periods ($\lesssim$60 min) and hydrogen-poor donors (see, e.g., Nelson et al. 1986; Nelemans & Jonker 2010; Tauris 2018; Chen et al. 2020).

MSPs are believed to be old radio pulsars with short spin periods ($<$30 ms) and weak surface magnetic fields ($\sim 10^8 - 10^9$ G), most of which are discovered in binaries (e.g., Lorimer 2008). In the standard recycling scenario, it has been thought that MSPs can be produced from the evolution of LMXBs, in which the NSs originated from core-collapse SNe (type Ib/Ic) and obtained sufficient mass from their companions, finally spinning up to millisecond periods (e.g., Chanmugam & Brecher 1987; Bhattacharya & van den Heuvel 1991). However, there is a discrepancy between the rates of Galactic LMXBs and MSPs for the standard recycling scenario (e.g, Kulkarni & Narayan 1988). Note that part of the current LMXBs and LMBPs may descend from the evolution of intermediate-mass X-ray binaries (IMXBs; e.g., Podsiadlowski et al. 2002; Li 2002, 2015).

As an alternative way to form MSPs, the AIC scenario could possibly help to explain the issue of rate of MSPs in the Galaxy (e.g., Bailyn & Grindlay 1990; Hurley et al. 2010). Tauris et al. (2013) suggested that ONe WDs with MS donors could form fully recycled MSPs with wider orbital periods ($\sim 10-60$ d; see also Hurley et al. 2010). By considering the irradiation-excited wind in accreting ONe WD binaries, Ablimit & Li (2015) found that ONe WDs with MS donors could naturally reproduce the formation of LMXBs with strong-field NSs like 4U 1822-37. They suggested that this channel can explain MSPs with He WD systems for orbital periods in the range of $\sim 0.1 - 30$ d. In recent years, with the increasing number of observed magnetic WDs, the magnetic field may play a key role in the evolution of WD binaries (e.g., Ablimit & Maeda 2019a,b). Under the assumptions of magnetic confinement scenario and evaporative winds, Ablimit (2019) recently argued that the AIC scenario is an alternative way to form two peculiar kinds of eclipsing MSPs, i.e., redbacks and black widows. For more studies on the formation of MSPs, see, e.g., Yoon & Langer (2005), Chen et al. (2013), Jia & Li (2014), Zhu et al. (2015), Smedley et al. (2017), Liu & Li (2017), etc.

2.2 The ONe WD+RG Channel

2.2.1 Evolutionary scenarios

In this channel, AIC events originate from the evolution of ONe WD+RG systems. There is one evolutionary scenario to form ONe WD+RG systems and then produce AIC events (see Fig. 3). Compared with the ONe WD+MS channel, AIC events in the ONe WD+RG channel originate from wider primordial binaries (e.g., Wang 2018a). The primordial primary fills its Roche lobe when it evolves to the thermally pulsing asymptotic giant branch (TPAGB) stage. In this case, the mass-transfer process is dynamically unstable and a CE may be formed. If the CE can be ejected, the primordial primary turns into an ONe WD. Subsequently, the primordial secondary continues to evolve and will become an RG star. At this moment, an ONe WD+RG system is formed. For this channel, the initial parameters of the primordial binaries for producing AIC events are in the range of $M_{1,\rm i} \sim 6-8.0\,M_\odot$, $q < 0.3$ and $P^{\rm i} \sim 1000 - 6000$ d.

2.2.2 Parameter space for AIC events

After the formation of ONe WD+RG systems, a CE may be easily formed when the RG star fills its Roche lobe, re-

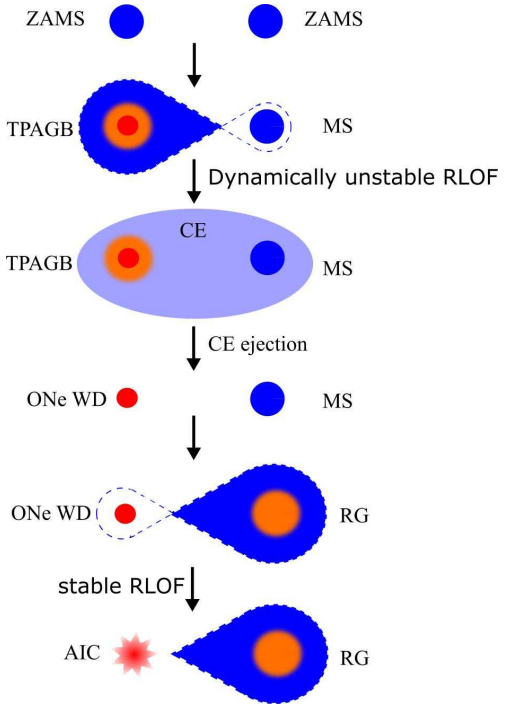

Fig. 3 Evolutionary scenario for ONe WD+RG systems that can form AIC events.

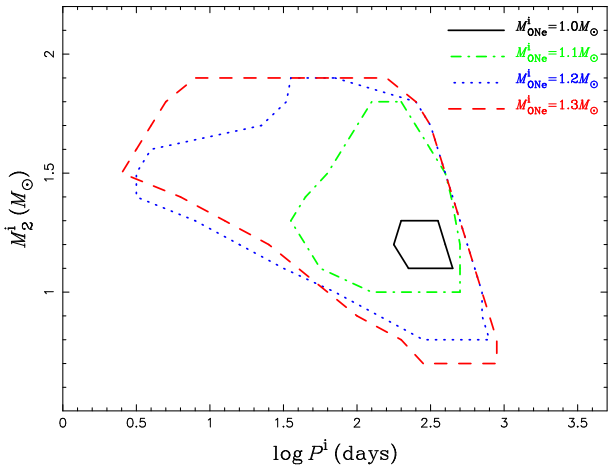

Fig. 4 Same as Fig. 2, but for the ONe WD+RG channel. Source: From Wang (2018a).

sulting in a small parameter space for producing WDs with $M_{\rm Ch}$ (e.g., Li & van den Heuvel 1997; Yungelson & Livio 1998). In order to stabilize the mass-transfer process and then to prevent the formation of the CE, Hachisu et al. (1999b) argued that the stellar wind from the WDs could strip some mass from the RG stars, but this mass-stripping scenario is still strongly debated and has not been confirmed by observations (e.g., Ablimit et al. 2014). By adopting a power-law adiabatic supposition for the mass-transfer prescription that can be applicable for the mass-transfer process from an RG donor (e.g., Ge et al. 2010), Liu et al. (2019) recently enlarged the parameter space of WD+RG systems for producing WDs with $M_{\rm Ch}$. It seems that the adiabatic mass-transfer prescription for RG donor is still highly uncertain (e.g., Woods & Ivanova 2011), but the work by Liu et al. (2019) at least provides an upper limit for the parameter regions that can form WDs with $M_{\rm Ch}$.

Figure 4 presents the initial parameter regions of AIC events for the ONe WD+RG channel in the $\log P^{\rm i} - M_2^{\rm i}$ plane with different $M^{\rm i}_{\rm ONe}$. In order to produce AIC events, the ONe WD should have RG companions with initial masses of $\sim 0.7 - 1.9\,M_\odot$ and initial orbital periods of $\sim 3{-}800$ d. The constraints on the boundaries of the initial regions in Figure 4 are similar to those of Figure 2. Note that some previous studies significantly extended the parameter space for forming WDs with $M_{\rm Ch}$, although their results are strongly dependent on the model assumptions (e.g., Lü et al. 2009; Chen et al. 2011c).

2.2.3 *Pre-AIC systems*

The pre-AIC systems with RG donors could potentially be identified as symbiotics in the observations. Symbiotics play a crucial role in the evolution of semi-detached/detached binaries. They are CO/ONe WD binaries with long orbital periods, usually consisting of a hot WD and an RG companion (see Truran & Cameron 1971). The hot WD could accrete H-rich matter from an evolved RG star through the RLOF process, but in most cases through the stellar wind of the RG star.

Symbiotic novae are a subclass of symbiotics, in which the mass accretor (CO/ONe WD) experiences a classical nova outburst. Many symbiotic novae have WD mass close to $M_{\rm Ch}$ with RG companions in observations, for example, T CrB (e.g., Belczyński & Mikołajewska 1998), RS Oph (e.g., Brandi et al. 2009; Mikołajewska & Shara 2017), V745 Sco (e.g., Drake et al. 2016; Orlando et al. 2017), J0757 (e.g., Tang et al. 2012), etc. Note that it is still not exclusively identified whether the WD in these symbiotic novae is an ONe WD or a CO WD.

2.2.4 *Post-AIC systems*

Compared with ONe WD+MS systems, the ONe WD+RG star systems could evolve to form more mildly recycled MSPs with He WD companions or even CO WD companions. The post-AIC systems with RG donors could potentially be identified as LMXBs and the resulting young MSPs with long orbital periods (> 500 d; see Tauris et al. 2013). For the ONe WD+RG star channel, the orbital period at the moment of the AIC and the orbit for the subsequent post-AIC systems (NS+RG systems) are relatively large. It has been suggested that such newborn NS bina-

ries with wide separations increase the possibility of disruption by stellar encounters in a globular cluster (e.g., Verbunt & Freire 2014; Belloni et al. 2020), possibly leading to the formation of isolated young NSs in globular clusters as suggested by Tauris et al. (2013).

2.3 The ONe WD+He Star Channel

2.3.1 Evolutionary scenarios

In this channel, AIC events originate from the evolution of ONe WD+He star systems. According to the evolutionary stage of the primordial primary when it first fills its Roche lobe, there are three evolutionary scenarios to form ONe WD+He star systems and then produce AIC events (see Fig. 5). Among the three scenarios, AIC events are mainly produced by Scenarios A and B, in which each scenario contributes about half of AIC events through the ONe WD+He star channel (see Wang 2018a).

Scenario A: The primordial primary first fills its Roche lobe at the HG or FGB, leading to a stable RLOF process. After the mass-transfer process, the primary becomes a He star and continues to evolve. Subsequently, the He star will exhaust its central He and expand quickly. The primary will fill its Roche lobe again at the He subgiant or He RG stage. In this case, the He-rich matter is transferred onto the surface of the secondary MS star in a stable way, after which an ONe SNe Ia system will be formed. The MS secondary continues to evolve and will fill its Roche lobe at the HG or FGB stage. At this stage, the mass-transfer is dynamically unstable and a CE may be formed. If the CE can be ejected, an ONe WD+He star system is formed. In this scenario, the initial parameters of the primordial binaries for producing AIC events are in the range of $M_{1,\rm i} \sim 6-11\,M_\odot$, $q > 0.2$ and $P^{\rm i} < 2500\,{\rm d}$. More than 40% of AIC events from the ONe WD+He star channel are produced through this scenario.

Scenario B: The primordial primary first fills its Roche lobe when it evolves to the EAGB or FGB stage, and transfers H-rich matter onto the surface of the secondary in a dynamically unstable way, leading to the formation of a CE. After the CE ejection, the primary becomes a He subgiant and continues to evolve. The primary will fill its Roche lobe again at the He RG stage and stably transfer He-rich matter onto the secondary MS star. Subsequently, the binary turns into an ONe SNe Ia system and will evolve to an ONe WD+He star system after experiencing the same evolutionary path as presented in Scenario A. For this scenario, the initial parameters of the primordial binaries for producing AIC events are in the range of $M_{1,\rm i} \sim 6-11\,M_\odot$, $q > 0.4$ and $P^{\rm i} \sim 300-6000\,{\rm d}$. More than half of AIC events from the ONe WD+He star channel are produced through this scenario.

Scenario C: The primordial primary first fills its Roche lobe when it evolves to the TPAGB stage and the primordial secondary evolves to the He-core burning stage. In this case, the mass-transfer is dynamically unstable and a CE with double cores will be formed. If the CE can be ejected, an ONe WD+He star system will be produced. In this scenario, the initial parameters of the primordial binaries for producing AIC events are in the range of $M_{1,\rm i} \sim 6-8\,M_\odot$, $q > 0.9$ and $P^{\rm i} \sim 800-6000\,{\rm d}$. Only about 5% of AIC events from the ONe WD+He star channel are produced through this scenario.

2.3.2 Parameter space for AIC events

After the formation of ONe WD+He star systems, the ONe WD could accrete He-rich matter from its He star companion once it fills its Roche lobe. The accreted He-rich matter is converted into C and O, enabling mass growth for the WD. The ONe WD may form an AIC event when it grows in mass close to $M_{\rm Ch}$. Figure 6 represents the initial parameter regions of ONe WD+He star systems that can lead to AIC events in the $\log P^{\rm i} - M_2^{\rm i}$ plane with different $M_{\rm ONe}^{\rm i}$. In order to produce AIC events, the ONe WD should have He star companions with initial masses of $\sim 0.8-3.3\,M_\odot$ and initial orbital periods of $\sim 0.04-1000\,{\rm d}$. The constraints on the boundaries of the initial regions in Figure 6 are similar to those of Figure 2.

2.3.3 Pre-AIC systems

In the observations, the pre-AIC systems with He star donors could potentially be identified as supersoft X-ray sources and He novae when the ONe WD accretes He-rich matter. (1) ONe WD+He star systems may appear as supersoft X-ray sources during the stable He-shell burning stage. The ONe WD will have a luminosity in the range of $10^{37}-10^{38}\,{\rm erg\,s^{-1}}$ when the He-shell burning is stable, consistent with that of the observed supersoft X-ray sources ($10^{36}-10^{38}\,{\rm erg\,s^{-1}}$; e.g., Kahabka & van den Heuvel 1997). (2) V445 Pup is a unique event discovered as a He nova so far, in which the WD had increased its mass close to $M_{\rm Ch}$ due to the accumulated material during nova outbursts (e.g., Ashok & Banerjee 2003; Kato et al. 2008; Woudt et al. 2009). It has been suggested that V445 Pup contains a CO WD but not an ONe WD due to no enhancement of Ne detected in the ejecta (see Woudt & Steeghs 2005). Thus, we speculate that V445 Pup may produce an SN Ia but not an AIC event.

2.3.4 Post-AIC systems

Compared with the LMBPs, intermediate-mass binary pulsars (IMBPs) include an NS and a massive CO/ONe WD.

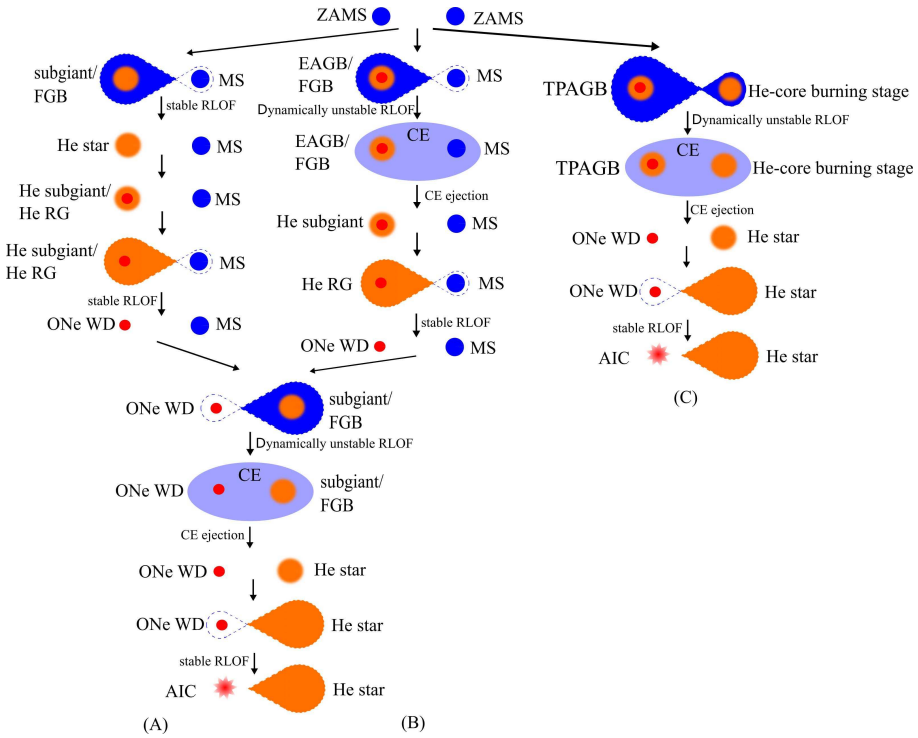

Fig. 5 Evolutionary scenarios for ONe WD+He star systems that can form AIC events.

The post-AIC systems with He star donors could potentially be identified as IMXBs and eventually produce IMBPs with short orbital periods. It has been suggested that most IMBPs may originate from IMXBs that consist of an NS and a $2-10\,M_{\odot}$ MS donor, known as the classic IMXB evolutionary scenario (e.g., Podsiadlowski et al. 2002; Tauris et al. 2012). However, Tauris et al. (2000) claimed that the IMXB evolutionary scenario is hard to form IMBPs with short orbital periods (<3 d). Note that the classic IMXB evolutionary scenario may also produce compact IMBPs when considering the effect of anomalous magnetic braking of Ap/Bp donors (e.g., Justham et al. 2006; Shao & Li 2012; Liu & Chen 2014).

Chen & Liu (2013) proposed an alternative evolutionary way (i.e., the NS+He star channel) to form IMBPs with short orbital periods (<3 d), but their work can only account for part of the observed IMBPs with short orbital periods (see also Tang et al. 2019). Liu et al. (2018a) recently studied the ONe WD+He star channel for the formation of IMBPs. They found that this channel may explain most of the observed IMBPs with short orbital periods. The studies by Liu et al. (2018a) can reproduce the observed parameters of PSR J1802-2124 well, which is one of the two precisely observed IMBPs.

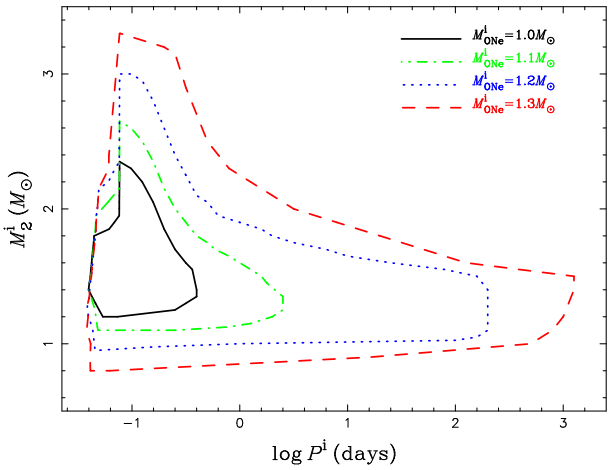

Fig. 6 Same as Fig. 2, but for the ONe WD+He star channel. Source: From Wang (2018a).

2.4 The CO WD+He Star Channel

2.4.1 Parameter space for AIC events

The CO WD+He star channel has been thought to be one of the promising ways to form the observed SNe Ia in young populations, in which a CO WD accretes He-rich matter from a He star once it fills its Roche lobe, leading to the mass-growth of the WD (e.g., Wang et al. 2009; Ruiter et al. 2009). Wang et al. (2017) recently found that

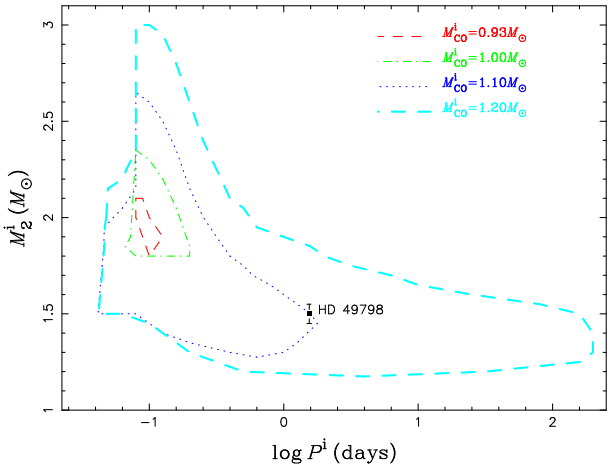

Fig. 7 Same as Fig. 2, but for the CO WD+He star channel. The *square with error bars* marks the location of HD 49798 with its massive WD companion (see Mereghetti et al. 2009). Source: From Wang (2018a).

if the mass-accretion rate is relatively high, the He-accreting CO WD will undergo off-center carbon ignition on its surface when it grows in mass close to $M_{\rm Ch}$ (see also Brooks et al. 2016). Previous studies usually supposed that the off-center carbon flame will reach the center of the CO WD, leading to the formation of an ONe WD that will collapse into an NS through the AIC process if the mass-transfer continues (e.g., Nomoto & Iben 1985; Saio & Nomoto 1985, 1998; Schwab et al. 2016). Note that there are three evolutionary scenarios to form CO WD+He star systems and then to produce WDs with $M_{\rm Ch}$ (for the details see Wang & Han 2012).

Figure 7 presents the initial parameter regions of CO WD+He star systems for producing AIC events in the $\log P^{\rm i} - M_2^{\rm i}$ plane with different $M_{\rm CO}^{\rm i}$. In this channel, the minimum $M_{\rm CO}^{\rm i}$ for the production of AIC events is $0.93\,M_\odot$. In order to produce AIC events, the CO WD should have He star companions with initial masses of $\sim 1.2-3\,M_\odot$ and initial orbital periods of $\sim 0.04-160$ d. The constraints on the upper and left/right-hand boundaries of the initial regions in Figure 7 are similar to those of Figure 2. The regions below the lower boundaries could produce SNe Ia due to the center carbon ignition when the WD grows in mass to $M_{\rm Ch}$ (see Wang et al. 2017). Note that some of the CO WD+He star systems beyond the right-hand boundaries can contribute to the formation of massive double CO WDs (e.g., Ruiter et al. 2013; Liu et al. 2018b).

It is still highly uncertain how the carbon flame propagates when off-center carbon ignition happens on the surface of CO WDs, leading to some uncertainties in the final fates of He-accreting CO WDs. Wu et al. (2020) recently studied the off-center carbon burning of He-accreting CO WDs by considering the effect of convective mixing. They argued that the temperature of the carbon flame is high enough to burn the carbon into silicon-group elements in the outer part of the CO core even though convective overshooting is considered. They suggested that the carbon flame will quench somewhere inside the CO WD, leading to the formation of a COSi WD that will explode as an SN Ia with Si-rich envelope if the mass accretion continues.

2.4.2 *Pre-AIC systems*

For the CO WD+He star channel, HD 49798 with its massive WD companion is a possible progenitor candidate of AIC events. HD 49798 is a $1.50 \pm 0.05\,M_\odot$ subdwarf O6 star that has a massive compact companion ($1.28 \pm 0.05\,M_\odot$) with an orbital period of 1.548 d (e.g., Thackeray 1970; Bisscheroux et al. 1997; Mereghetti et al. 2009). Krtička et al. (2019) recently derived the mass of HD 49798 as $1.46 \pm 0.32\,M_\odot$ based on the spectroscopic surface gravity, which is in agreement with the mass obtained from the orbital solution by Mereghetti et al. (2009). The binary parameters of HD 49798 with its companion are located in the initial contours of CO WD+He star systems for the production of AIC events (see Fig. 7). Thus, we speculate that the WD companion of HD 49798 may collapse into an NS eventually. Note that it is still highly uncertain whether the companion of HD 49798 is an ONe WD or a CO WD (e.g., Liu et al. 2015; Mereghetti et al. 2016; Popov et al. 2018).

2.4.3 *Post-AIC systems*

CO WD+He star systems could form ONe WD+He star systems due to off-center carbon burning happening on the surface of the He-accreting CO WD if the mass-transfer rate is relatively high (see Wang et al. 2017). After that, the ONe WD+He star systems continue to evolve and form NS+He star systems if AIC happens, in which the newborn NS may be recycled when the He star refills its Roche lobe again. Similar to the ONe WD+He star channel, the post-AIC systems with He star donors could potentially be identified as IMXBs, finally leading to the formation of IMBPs.

3 THE DOUBLE-DEGENERATE MODEL

Close double WDs are the outcomes of low-/intermediate-mass binaries, playing a key role in modern astrophysics. They are expected to be potential low-frequency GW emission sources in the Galaxy (see Sect. 4.3) and contain important information for the constraints on CE evolution (e.g., Han 1998; Nelemans et al. 2001a). In the classic double-degenerate model of AIC events, a WD merges with another WD in a compact binary with total mass

heavier than $M_{\rm Ch}$, finally forming an AIC event (e.g., Lyutikov & Toonen 2017; Ruiter et al. 2019; Liu & Wang 2020). The classic double-degenerate model mainly involves the merger of double CO WDs (the double CO WD channel), the merger of double ONe WDs (the double ONe WD channel) and the merger of ONe WD+CO WD systems (the ONe WD+CO WD channel). In addition, an alternative way could be the merging of a WD with a core of an asymptotic giant branch (AGB) star during the CE evolution, then in a short or long time leading to AIC (e.g., Sabach & Soker 2014; Canals et al. 2018; Soker et al. 2019).

For the mergers of double CO WDs, there is some parameter space to produce AIC events (see Sect. 3.1.2). For the mergers of double ONe WDs and ONe WD+CO WD systems, the primary ONe WD will collapse into an NS, resulting from the electron-capture reactions by Mg and Ne (e.g., Nomoto & Iben 1985; Saio & Nomoto 1985; Wu & Wang 2018). The merging of double WDs may also relate to some high-energy events, such as high-energy neutrino emission and short gamma-ray bursts (e.g., Xiao et al. 2016; Lyutikov & Toonen 2017; Rueda et al. 2019). Kashyap et al. (2018) recently argued that the mergers of ONe WD+CO WD systems might also form very faint and rapidly fading SNe Ia through a failed detonation. Liu & Wang (2020) recently studied the formation of AIC events through the merging of different kinds of double WDs in a systematic way. For more studies on the double-degenerate model of AIC events, see, e.g., Lyutikov & Toonen (2017) and Ruiter et al. (2019).

Aside from the contribution to single NSs via AIC, the merging of double WDs may also relate to the formation of some other important peculiar objects based on the underlying compositions of the two WDs, for example, SNe Ia via the merging of double CO WDs (e.g., Webbink 1984; Iben & Tutukov 1984) or the merging of CO WD+He-rich WD (e.g., Dan et al. 2012; Liu et al. 2017; Crocker et al. 2017), single hot subdwarfs via the merging of double He WDs (e.g., Han et al. 2003; Zhang & Jeffery 2012), R Coronae Borealis (R CrB) stars and extreme He stars via the merging of CO WD+He WD (e.g., Webbink 1984; Iben & Tutukov 1984; Zhang et al. 2014), or some Ca-rich transients (i.e., subluminous 2005E-like SNe) via the merging of low-mass CO WD+He WD (e.g., Perets et al. 2010; Meng & Han 2015), etc. Note that AM Canum Venaticorum (AM CVn) binaries may originate from the evolution of CO WD+He WD systems (e.g., Warner 1995; Nelemans et al. 2001b) or double He WDs (see Zhang et al. 2018).

3.1 The Double CO WD Channel

3.1.1 Evolutionary scenarios

There are three classic binary evolutionary scenarios to form double CO WDs that have total mass $\geq M_{\rm Ch}$ and merge in the Hubble time (see fig. 11 of Wang 2018b). For Scenario A, the initial parameters of the primordial binaries for producing AIC events are in the range of $M_{1,\rm i} \sim 3-9\,M_\odot$, $q > 0.2$ and $P^{\rm i} < 1500\,{\rm d}$. For Scenario B, the initial binary parameters are in the range of $M_{1,\rm i} \sim 3-7\,M_\odot$, $q > 0.3$ and $P^{\rm i} \sim 1300-5000\,{\rm d}$. For Scenario C, the initial binary parameters are in the range of $M_{1,\rm i} \sim 3-7\,M_\odot$, $q > 0.5$ and $P^{\rm i} \sim 400-5000\,{\rm d}$. In Scenario C, the double WDs can also be formed after the first CE ejection directly in some cases. Among the three scenarios, AIC events are mainly produced by Scenarios A and B, in which each scenario contributes to about 40% of AIC events (see Liu & Wang 2020). For more discussions on the formation of double CO WDs, see previous studies (e.g., Han 1998; Nelemans et al. 2001a; Ruiter et al. 2009, 2013; Toonen et al. 2012; Yungelson & Kuranov 2017).

The binary evolutionary paths in figure 11 of Wang (2018b) originate from the CE ejection process before the formation of double CO WDs, known as the CE ejection scenarios. Ruiter et al. (2013) proposed an important phase to simulate the formation of double CO WDs, in which the primary CO WD is able to grow in mass by accreting He-rich matter from a He subgiant companion before forming a double CO WD system, called the CO WD+He subgiant scenario (see also Liu et al. 2016, 2018b). Compared with the CE ejection scenario, the mass-transfer process before the production of double CO WDs is stable for the CO WD+He subgiant scenario that allows forming massive primary CO WDs and thus more massive double CO WDs. Liu et al. (2018b) recently found that the CO WD+He subgiant scenario has a significant contribution to the formation of massive double CO WDs that may have He-rich atmospheres (double DB/DO WDs in the observations). By using Sloan Digital Sky Survey (SDSS) and Gaia data, Genest-Beaulieu & Bergeron (2019) recently discovered 55 unresolved double DB WDs, which are observational evidence to support the WD+He subgiant scenario for producing massive double WDs.

3.1.2 Parameter space for AIC events

The merging of double CO WDs has been thought to be one of the two major pathways for the formation of SNe Ia (e.g., Webbink 1984; Iben & Tutukov 1984). However, some previous studies suggested that the merging of double CO WDs may also lead to the formation of NSs via the AIC process; off-center carbon burning may occur

on the surface of the massive CO WD due to a relatively rapid mass-transfer process during the merging, likely converting CO WDs into ONe WDs through an inwardly propagating carbon flame (e.g., Nomoto & Iben 1985; Saio & Nomoto 1985, 1998; Timmes et al. 1994). Pakmor et al. (2010) suggested that the AIC may be avoided when the coalescence process is violent, in which a prompt detonation is triggered if the merging continues, resulting in the formation of an SN Ia but not an AIC event (known as the violent merger scenario). Pakmor et al. (2011) argued that the mass-ratio of double CO WDs may have a significant influence on their final fates. They suggested that the minimum critical mass-ratio for the violent merger scenario is ∼0.8 (see also Sato et al. 2016). This indicates that AIC events are likely to be formed when the mass-ratio of double CO WDs is < 0.8.

Wu et al. (2019) recently found that the outcomes of double CO WDs mainly depend on the merging processes (e.g., violent merger, fast merger, slow merger, composite merger, etc). On the basis of the thick-disk assumption (i.e., slow merger), Wu et al. (2019) found that the final evolutionary fates of double CO WDs are strongly dependent on the mass-accretion rate during the merging, which can be divided into four regions: (1) off-center O/Ne ignitions, then off-center explosion or Si-Fe cores; (2) ONe cores, then NSs via AIC; (3) OSi cores, then core-collapse SNe; (4) explosive carbon ignition in the center, then SNe Ia. They also found that the influence of initial WD mass and cooling time on the final fates of double CO WDs can be ignored. Compared with the violent merger scenario (e.g., Pakmor et al. 2010, 2011; Sato et al. 2016), the slow merger scenario adopted by Wu et al. (2019) allows a low mass-ratio ($< 2/3$) for double WDs, in which stable mass-transfer can occur[2]. Note that the outcomes of double CO WDs are still under debate, for more discussions, see, e.g., Han & Webbink (1999), Yoon et al. (2007), Chen et al. (2012), Kromer et al. (2013), Taubenberger et al. (2013), Moll et al. (2014), Tanikawa et al. (2015), Fesen et al. (2015), Bulla et al. (2016), etc.

3.1.3 Progenitor candidates

Henize 2–428 and KPD 1930+2752 are two massive WDs that can merge in the Hubble time. (1) Henize 2-428 is a bipolar planetary nebula with a double-degenerate core. Santander-García et al. (2015) suggested that the nucleus of Henize 2-428 contains a double CO WD, which has a total mass $\sim 1.76\,M_\odot$ and mass-ratio ∼1 with an orbital period of ∼4.2 h. On the basis of the violent merger scenario, the final fate of Henize 2-428 may be an SN Ia but not an AIC event. (2) KPD 1930+2752 is a CO WD+sdB binary, which has a total mass $\sim 1.36-1.48\,M_\odot$ and a $\sim 0.45-0.52\,M_\odot$ sdB star with an orbital period of ∼2.28 h (e.g., Maxted et al. 2000; Geier et al. 2007). Liu et al. (2018b) recently suggested that KPD 1930+2752 will form a double WD in ∼200 Myr due to the evolution of the sdB star, after which it will merge in ∼4 Myr. The final fate of KPD 1930+2752 may be an AIC event as its mass-ratio is far below 0.8.

Meanwhile, there are some other massive double WDs in the observations that may have total mass close to $M_{\rm Ch}$, e.g., GD 687 (e.g., Geier et al. 2010), SBS 1150+599A (see Tovmassian et al. 2010), V458 Vulpeculae (see Rodríguez-Gil et al. 2010), WD 2020-425 (see Napiwotzki et al. 2007), NLTT 12758 (Kawka et al. 2017), etc. Hollands et al. (2020) recently reported the identification of a $1.14\,M_\odot$ WD, i.e., WD J0551+4135. They argued that the ultra-massive WD with a unique hydrogen/carbon mixed atmosphere is consistent with the merger remnant of double WDs in a tight binary. In addition, Borges et al. (2020) argued that the anomalous X-ray pulsar 4U 0142+61 may harbor a fast-rotating magnetic young WD with mass near $M_{\rm Ch}$, which can be the recent outcome of the merging from two less massive WDs. It has been proposed that continuous GW emission may be one of the probes to detect ultra-massive WDs directly by various future space-based detectors (see Kalita et al. 2020).

Some systematic surveys have been proposed to search for double WDs, e.g., the SWARMS survey (e.g., Badenes et al. 2009) and the ESO SN Ia Progenitor Survey (SPY; e.g., Koester et al. 2001; Napiwotzki et al. 2004; Nelemans et al. 2005; Geier et al. 2007). Carrasco et al. (2014) estimated that a large number of double WDs may be discovered by Gaia (see also Toonen et al. 2017). Tian et al. (2020a) recently provided hundreds of double WDs and more than ten thousand WD+MS binaries selected from Gaia Data Release 2 (DR2). In addition, the GPS1 (see Tian et al. 2017) and its extended proper motion catalogs (GPS1+; see Tian et al. 2020b) could provide a more substantial population of WD binaries due to its accurate photometric and astrometric data from Gaia DR1 (DR2), PS1, SDSS and 2MASS.

3.2 The Double ONe WD Channel

According to the evolutionary stage of the primordial primary when it first fills its Roche lobe, there are three evolutionary scenarios to form double ONe WDs that can produce AIC events (see Fig. 8), in which Scenario A is the main way to form AIC events (see Liu & Wang 2020).

[2] In the slow merger scenario, the less massive WD will be tidally disrupted and form a pressure-supported disk around the massive WD; the mass-accretion rate from the disk onto the massive WD is around the Eddington rate and the accreting process can last for millions of years (e.g., Saio & Jeffery 2000, 2002).

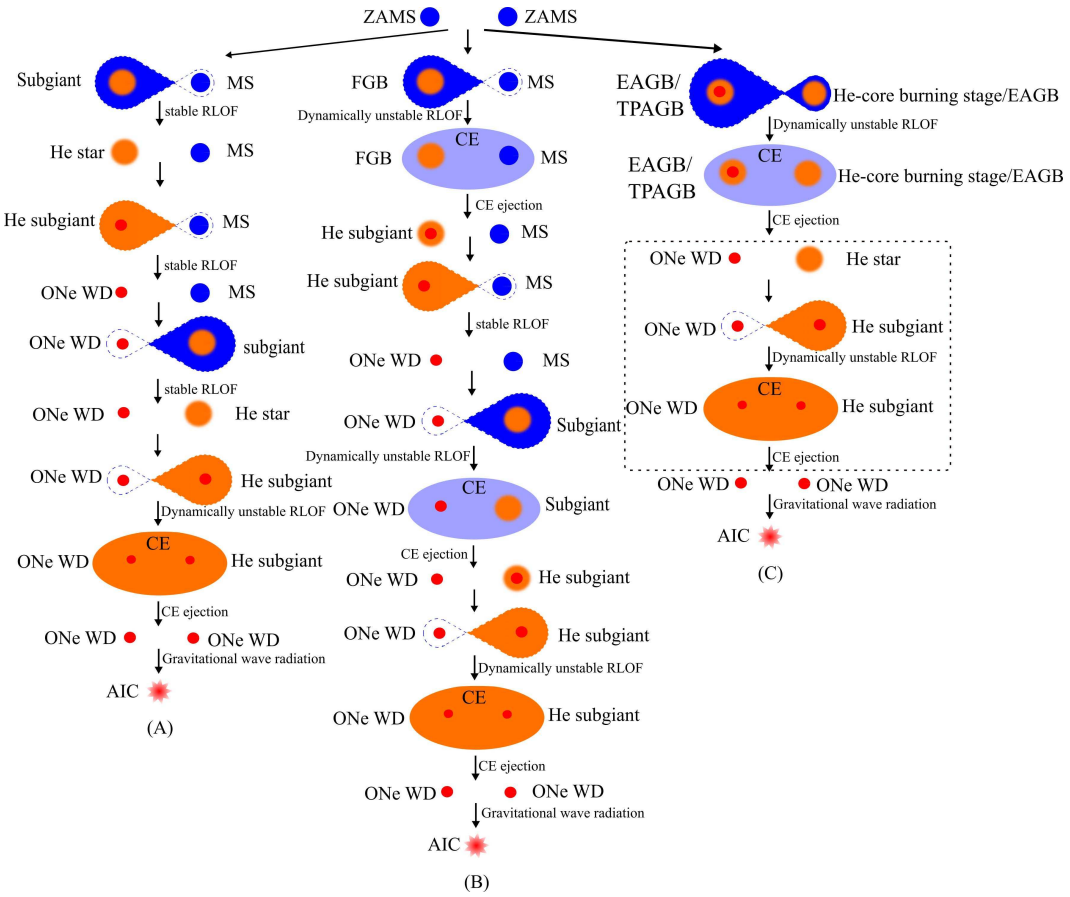

Fig. 8 Evolutionary scenarios to double ONe WDs that can form AIC events. In Scenario C, some cases will not experience the second CE ejection (*dashed box*).

Scenario A: The primordial primary first fills its Roche lobe at the HG stage and transfers H-rich matter stably onto the secondary. After the mass-transfer process, the primary turns into a He star and continues to evolve. The He star will fill its Roche lobe again when its central He is exhausted and evolve to be a He subgiant. In this case, the He subgiant stably transfers He-rich matter onto the MS secondary, after which the primary becomes an ONe WD. Subsequently, the primordial secondary will fill its Roche lobe at the HG stage and start a stable RLOF process. After that, the secondary evolves to a He star and continues to evolve. The secondary would fill its Roche lobe again when its central He is exhausted and evolve to a He subgiant. In this case, the mass-transfer is dynamically unstable and a CE may be formed. After the CE ejection, the secondary becomes another ONe WD, i.e., a double ONe WD system is formed. For this scenario, the initial parameters of the primordial binaries for producing AIC events are in the range of $M_{1,\mathrm{i}} \sim 8-11\,M_{\odot}$, $q \sim 0.2-0.8$ and $P^{\mathrm{i}} < 40\,\mathrm{d}$. About 78% of AIC events from the double ONe WD merger channel are produced through this scenario.

Scenario B: The primordial primary first fills its Roche lobe at the FGB phase, and transfers H-rich matter onto the surface of the secondary. In this case, the mass-transfer process is dynamically unstable and a CE would be formed. If the CE can be ejected, the primary turns into a He subgiant. The He subgiant will quickly fill its Roche lobe again and stably transfer He-rich matter onto the MS secondary. After the mass-transfer process, the binary becomes an ONe SNe Ia system. Subsequently, the primordial secondary will evolve to the HG stage and fill its Roche lobe. In this case, the mass-transfer is dynamically unstable and a CE may be formed. After the CE ejection, the secondary becomes a He subgiant and will fill its Roche lobe again. At this stage, the mass-transfer is also dynamically unstable and a CE will be formed. If the CE can be ejected, a double ONe WD system will be produced. In this scenario, the initial parameters of the primordial binaries for producing AIC events are in the range of $M_{1,\mathrm{i}} \sim 8-11\,M_{\odot}$, $q > 0.7$ and $P^{\mathrm{i}} \sim 500-1000\,\mathrm{d}$. About 7% of AIC events from the double ONe WD merger channel are produced through this scenario.

Scenario C: The primordial primary fills its Roche lobe when it evolves to the EAGB or TPAGB phase and the primordial secondary evolves to the He-core burning stage or the EAGB stage. In this case, a CE may be formed due to the dynamically unstable mass-transfer. After the CE ejection, an ONe WD+He star system will be produced. The He star continues to evolve and will evolve to a He subgiant when its central He is exhausted. At this stage, the He subgiant will expand quickly and fill its Roche lobe. The second CE may be formed because of dynamically unstable RLOF. If the CE can be ejected, a double ONe WD system will be produced. Note that the second CE evolution process displayed in the dashed box in Figure 8 may not be indispensable in some cases. For this scenario, the initial parameters of the primordial binaries for producing AIC events are in the range of $M_{1,\rm i} \sim 6-9\,M_\odot$, $q>0.8$ and $P^{\rm i} \sim 400-6000\,{\rm d}$. About 15% of AIC events from the double ONe WD channel are produced through this scenario.

3.3 The ONe WD+CO WD Channel

According to the evolutionary stage of the primordial primary when it first fills its Roche lobe, there are three evolutionary scenarios to form ONe WD+CO WD systems and then merge to produce AIC events (see Fig. 9), in which Scenario A is the main way to form AIC events (see Liu & Wang 2020). In Scenario A, the primordial primary evolves to a CO WD first and then the primordial secondary forms an ONe WD, whereas it will be the other way around for Scenarios B and C.

Scenario A: The primordial primary first fills its Roche lobe at the HG stage and stably transfers H-rich matter onto the surface of the primordial secondary, leading to a mass reversal of the binary, i.e., an Algol binary is formed. After the mass-transfer process, the primordial primary turns into a He star and continues to evolve. The He star will exhaust its central He and evolve to a He RG. At this stage, the He star will expand quickly and fill its Roche lobe again. The primordial primary stably transfers He-rich matter onto the secondary. After the stable RLOF, the binary becomes a CO SNe Ia system. Subsequently, the primordial secondary fills its Roche lobe at the HG or FGB stage and experiences a stable RLOF process. After that, the primordial secondary becomes a He subgiant and will fill its Roche lobe again. In this case, a CE may be formed due to the dynamically unstable RLOF. If the CE can be ejected, an ONe WD+CO WD system will be produced. In this scenario, the initial parameters of the primordial binaries for producing AIC events are in the range of $M_{1,\rm i} \sim 4-11\,M_\odot$, $q>0.2$ and $P^{\rm i}<1000\,{\rm d}$. About half of AIC events from the ONe WD+CO WD merger channel are produced through this scenario.

Scenario B: The primordial primary fills its Roche lobe when it evolves to the EAGB phase, leading to the formation of a CE due to the dynamically unstable RLOF. If the CE can be ejected, the primordial primary becomes a He subgiant and continues to evolve. The He subgiant will fill its Roche lobe quickly and transfer He-rich matter onto the MS secondary stably. After the mass-transfer process, the binary turns to be an ONe SNe Ia system. Subsequently, the secondary will fill its Roche lobe at the HG phase, and transfer H-rich matter onto the surface of the ONe WD. In this case, the mass-transfer is dynamically unstable and a CE may be formed. After the CE ejection, an ONe WD+He subgiant system will be produced. The He subgiant will quickly fill its Roche lobe again, and transfer He-rich matter onto the ONe WD. At this stage, the second CE may be formed due to the dynamically unstable RLOF. If the CE can be ejected, an ONe WD+CO WD system will be formed finally. Note that the third CE evolution process illustrated in the dashed box in Figure 9 may not be indispensable in some cases. In this scenario, the initial parameters of the primordial binaries for producing AIC events are in the range of $M_{1,\rm i} \sim 2-11\,M_\odot$, $q>0.2$ and $P^{\rm i} \sim 400-6000\,{\rm d}$. About 30% of AIC events from the ONe WD+CO WD merger channel are produced through this scenario.

Scenario C: The primordial primary first fills its Roche lobe when it evolves to the TPAGB phase. In this case, the mass-transfer is dynamically unstable and a CE may be formed. After the CE ejection, an ONe SNe Ia system is produced. Subsequently, the binary will evolve to an ONe WD+CO WD system after experiencing similar evolution as presented in Scenario B. In this scenario, the initial parameters of the primordial binaries for producing AIC events are in the range of $M_{1,\rm i} \sim 5-9\,M_\odot$, $q>0.3$ and $P^{\rm i} \sim 200-1600\,{\rm d}$. About 20% of AIC events from the ONe WD+CO WD merger channel are produced through this scenario.

4 BINARY POPULATION SYNTHESIS

Binary population synthesis is a useful approach to simulate a large population of stars or binaries, especially for the formation of peculiar stars, and then to compare the theoretical results with those of observations (e.g., Han et al. 1995; Yungelson & Livio 1998; Nelemans et al. 2001a,b; Hurley et al. 2010). Table 1 presents the estimated Galactic rates, NS numbers and delay times of AIC events from various channels with different CE ejection parameters. The estimated Galactic rates of AIC events are strongly dependent on the value of the CE ejection param-

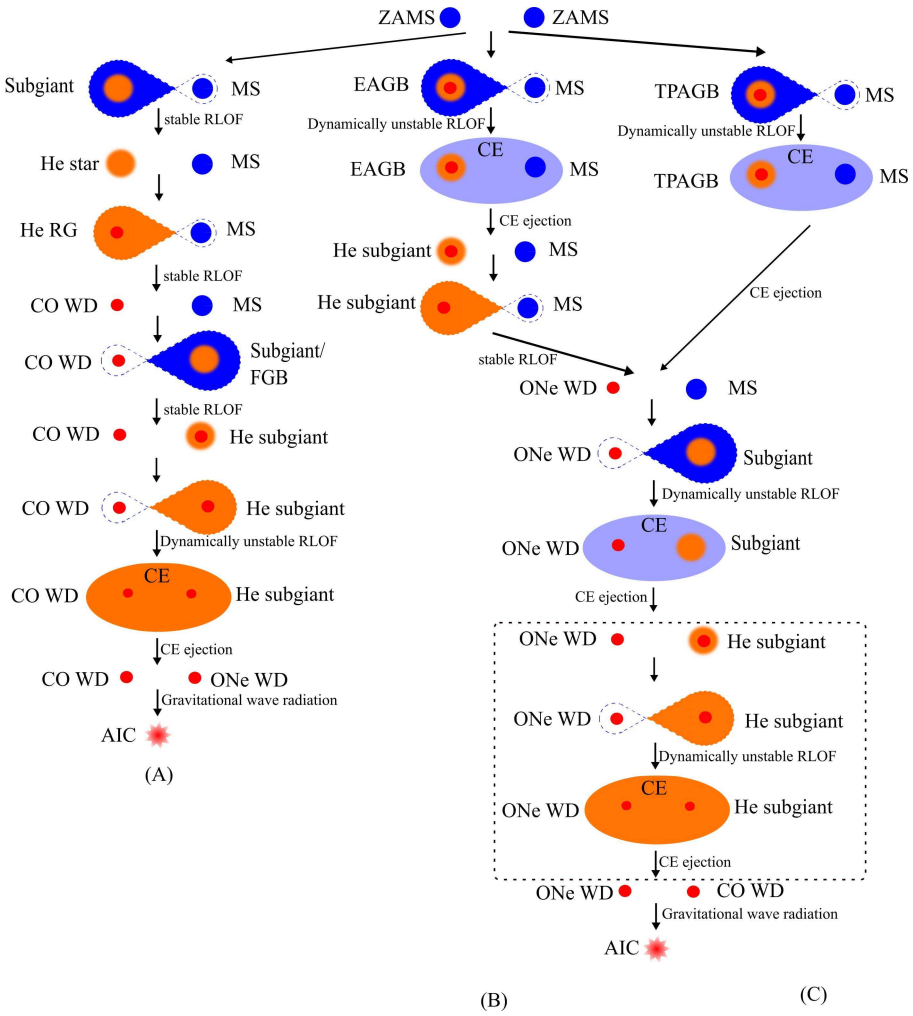

Fig. 9 Evolutionary scenarios for ONe WD+CO WD systems that can form AIC events. In Scenarios B and C, some cases will not experience the third CE ejection (*dashed box*).

eter $\alpha_{\rm CE}\lambda$ that is still highly uncertain (e.g., Ivanova et al. 2013).

4.1 Predicted Rates of AIC Events

Figure 10 depicts the evolution of AIC rates changing with time in the Galaxy. The estimated rates of AIC events in the Galaxy are in the range of $\sim 0.3-0.9\times 10^{-3}\,{\rm yr}^{-1}$ for the single-degenerate model and $\sim 1.4-8.9\times 10^{-3}\,{\rm yr}^{-1}$ for the double-degenerate model, in which the double-degenerate model plays a dominant role. Fryer et al. (1999) estimated that the rates of AIC events range from $10^{-7}-10^{-5}\,{\rm yr}^{-1}$ by modeling the r-process nucleosynthetic yields of neutron-rich ejecta through the AIC process. Although it is still under debate whether the AIC process produces the r-process elements or not (e.g., Fryer et al. 1999; Qian & Wasserburg 2007), the theoretical AIC rates in this review at least provide an upper limit for the AIC events.

The estimated Galactic number of NS systems originating from the single-degenerate model may be in the range of $\sim 0.4-1.1\times 10^7$, and the single NS number from the double-degenerate model ranges from $\sim 0.2-1.1\times 10^8$. In the single-degenerate model, the ONe WD+He star channel is the main way to produce AIC events, and we cannot ignore the contribution of the CO WD+He star channel when studying AIC events. In the double-degenerate model, the double CO WD channel plays a main role in the formation of AIC events though some uncertainties for this channel exist. If we did not consider the contribution of double CO WD mergers, the Galactic rates of AIC events from the double-degenerate model will decrease to $\sim 0.6-4.7\times 10^{-3}\,{\rm yr}^{-1}$, and the corresponding single NS number decreases to $\sim 0.4-4.5\times 10^7$.

Lyutikov & Toonen (2017) recently investigated the formation of AIC events from the merging of ONe WD+CO WD systems in a systematic way. The predicted rates of AIC events in Table for the ONe WD+CO WD

Table 1 The Estimated Galactic Rates, NS Numbers and Delay Times of AIC Events for Various Channels with Different Values of CE Ejection Parameters

Channels	$\alpha_{\rm CE}\lambda$	$\nu_{\rm AIC}$ ($10^{-3}\,{\rm yr}^{-1}$)	Number (10^7)	Delay Times (Myr)
ONe WD+MS	0.5	0.138	0.165	$110-1400$
ONe WD+MS	1.5	0.079	0.095	$70-1400$
ONe WD+RG	0.5	0.012	0.014	$1400-6300$
ONe WD+RG	1.5	0.033	0.040	$1400-6300$
ONe WD+He star	0.5	0.105	0.126	$40-140$
ONe WD+He star	1.5	0.676	0.811	$30-180$
CO WD+He star	0.5	0.083	0.100	$50-110$
CO WD+He star	1.5	0.129	0.155	$50-110$
Double CO WDs	0.5	1.129	1.356	>90
Double CO WDs	1.5	5.160	6.194	>110
Double ONe WDs	0.5	0.051	0.061	>55
Double ONe WDs	1.5	0.285	0.342	>55
ONe WD+CO WD	0.5	0.268	0.321	>55
ONe WD+CO WD	1.5	3.486	4.184	>55

We adopt metallicity $Z = 0.02$ and a constant star-formation rate of $5\,M_\odot\,{\rm yr}^{-1}$ in our Galaxy. The results for different single-degenerate models are from Wang (2018a), whereas the results for different double-degenerate models are from Liu & Wang (2020).
Notes: $\alpha_{\rm CE}\lambda$ = CE ejection parameter; $\nu_{\rm AIC}$ = Galactic rates of AIC events; Number = Expected number of NS systems from the single-degenerate model or single isolated NSs from the double-degenerate model in the Galaxy.

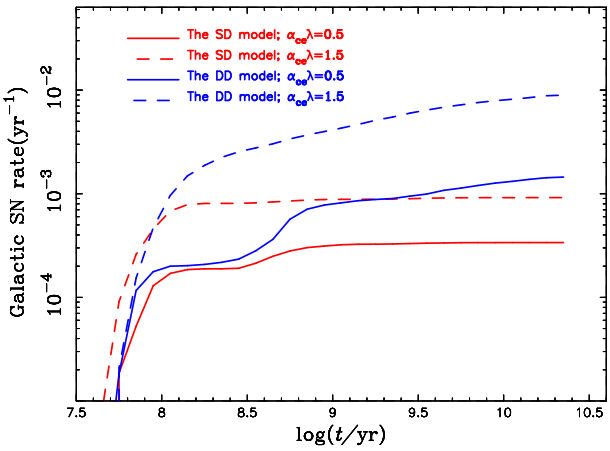

Fig. 10 Evolution of the predicted AIC rates as a function of time in the Galaxy for the single-degenerate and double-degenerate models with different $\alpha_{\rm CE}\lambda$ by adopting metallicity $Z = 0.02$ and a constant star-formation rate of $5\,M_\odot\,{\rm yr}^{-1}$. The results for the single-degenerate model are from Wang (2018a), whereas the results for the double-degenerate model are from Liu & Wang (2020).

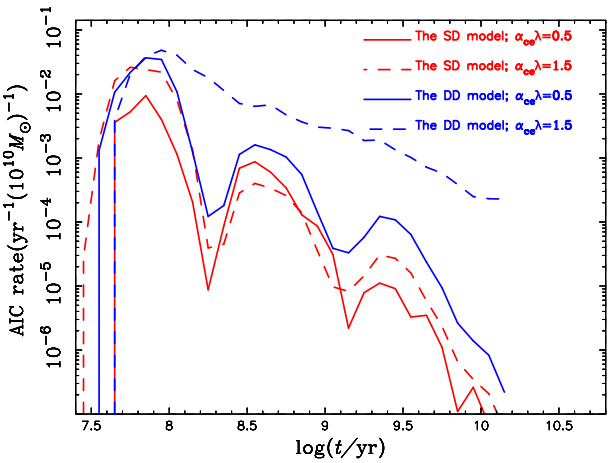

Fig. 11 Delay time distributions of AIC events based on a single starburst with a total mass of $10^{10}\,M_\odot$. The results for the single-degenerate model are from Wang (2018a), whereas the results for the double-degenerate model are from Liu & Wang (2020).

channel are compatible with those of Lyutikov & Toonen (2017) if a small value of $\alpha_{\rm CE}\lambda$ is adopted. Employing a binary population synthesis method, Ruiter et al. (2019) recently systematically studied the single-/double-degenerate models of AIC events. The predicted Galactic rates of AIC events in this review are somewhat higher than those of Ruiter et al. (2019). The main reason is that Ruiter et al. (2019) did not consider the contribution of the CO WD+He star channel in the single-degenerate model and the double CO WD channel in the double-degenerate model.

The delay times of AIC events represent the time interval from star formation to the occurrence of AIC. Figure 11 presents the delay time distributions of AIC events based on a single starburst with a total mass of $10^{10}\,M_\odot$ in stars. In the single-degenerate model, the ONe/CO WD+He star channels mainly contribute to AIC events with short delay times after the starburst, the ONe WD+MS channel to the intermediate delay times and the ONe WD+RG channel to the long delay times. AIC events with the shortest delay

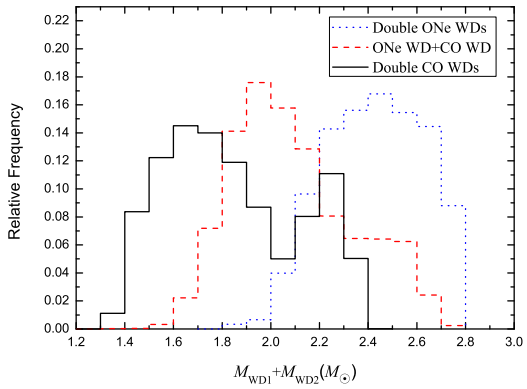

Fig. 12 The total mass distributions of different kinds of double WD mergers for producing AIC events with $\alpha_{\rm CE}\lambda = 1.0$. The data points forming these distributions are from Liu & Wang (2020).

times have a He star donor at the moment of NS formation, and the corresponding post-AIC systems with He star donors may eventually produce IMBPs with short orbital periods (see Sects. 2.3.4 and 2.4.3). AIC events with the longest delay times have an RG donor at the moment of NS formation, and most of the post-AIC systems with RG donors will finally form NS+He WD systems with long orbital periods, which may be identified as young MSPs in globular clusters (see Sect. 2.2.4). The double-degenerate model will produce AIC events from 55 Myr to the Hubble time, which is determined by the merging timescale of double WDs resulting from GW emission. The minimum delay time in Figure 11 is mainly determined by the MS lifetime of the maximum mass of a star forming an ONe WD, depending on the change in metallicities (e.g., Doherty et al. 2017).

4.2 Mass Distribution of NSs

The post-AIC events from the single-degenerate model could potentially be identified as low/intermediate-mass X-ray binary pulsars, and then the resulting low/intermediate-mass binary pulsars that may have NSs with masses in the range of $\sim 1.25 - 1.7\,M_\odot$ (e.g., Tauris et al. 2013; Liu et al. 2018a). However, the NSs resulting from the double-degenerate model are quite different from those of the single-degenerate model. The merging of double WDs will form single isolated NSs with a large mass range after the AIC process. Compared with the single NSs originating from classic core-collapse SNe, single NSs from the mergers of double WDs may correspond to a specific kind of NSs, exhibiting some different properties, such as circumstellar environments, magnetic fields, etc. Beznogov et al. (2020) recently suggested that NSs originating from AIC may be observable during the neo-NS (i.e., hot NS) stage, in which the NS has just become transparent to neutrinos. For more studies on isolated NSs, see, e.g., Tauris & van den Heuvel (2006), Popov (2011), Liu & Li (2019), Soker (2020), Jiang et al. (2020), etc.

Figure 12 presents the total mass distribution of different double WD mergers for producing AIC events. The total masses of double WD mergers are mainly in the range of $\sim 1.4 - 2.8\,M_\odot$, which at least provides an upper limit for the maximum mass of the formed single isolated NSs. Currently, the most reliable constraints on the maximum mass of NSs are from the mass determinations of the massive pulsar binaries in the observations, e.g., PSR J0740+6620 with $M_{\rm NS} = 2.14^{+0.10}_{-0.09}\,M_\odot$ (see Cromartie et al. 2020), PSR J0348+0432 with $M_{\rm NS} = 2.01 \pm 0.04\,M_\odot$ (see Antoniadis et al. 2013) and PSR J1614-2230 with $M_{\rm NS} = 1.97 \pm 0.04\,M_\odot$ (Demorest et al. 2010). These observational values provide a lower limit on the maximum mass of NSs.

For the double-degenerate model of AIC events, the total merging masses are mainly in the range of $1.4 - 2.4\,M_\odot$ for the mergers of double CO WDs, $2.0 - 2.8\,M_\odot$ for the mergers of double ONe WDs and $1.6 - 2.7\,M_\odot$ for the mergers of ONe WD+CO WD systems. The total mass distributions in Figure 12 have two peaks for the double CO WD mergers, in which the left peak mainly originates from the classic CE ejection scenarios (see fig. 11 of Wang 2018b), and the right peak mainly originates from the CO WD+He subgiant scenario that can make the primary CO WDs grow in mass up to $0.48\,M_\odot$ after its formation (see Liu et al. 2018b).

4.3 Gravitational Wave Signals

After the detection of the first double black hole merger by the ground-based aLIGO/Virgo, many double black hole mergers and one double NS merger have been confirmed in the past few years, starting a new era in GW astronomy (e.g., Abbott et al. 2016, 2017a,b). Close double WDs with short orbital periods are expected to dominate the Galactic GW background in the range of $10^{-4} - 10^{-1}$ Hz (e.g., Evans et al. 1987; Nelemans et al. 2001a). They would be observable by future space-based GW detectors, such as the Laser Interferometer Space Antenna (LISA; e.g., Nelemans et al. 2004; Ruiter et al. 2010; Marsh 2011), TianQin (e.g., Luo et al. 2016; Wang et al. 2019; Bao et al. 2019; Shi et al. 2019; Feng et al. 2019), Taiji (e.g., Ruan et al. 2019, 2020a,b; Luo et al. 2020), etc. Nelemans (2013) estimated that several thousand double WDs should be individually detected by LISA.

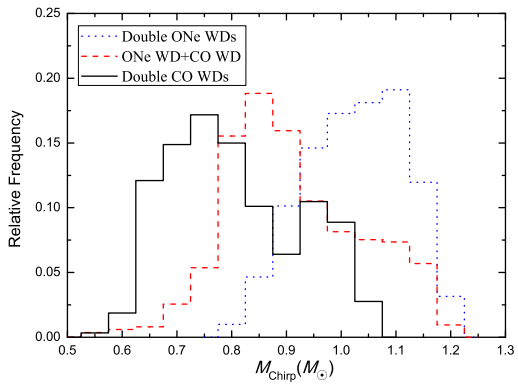

Fig. 13 Chirp mass distributions of different kinds of double WDs for producing AIC events with $\alpha_{\rm CE}\lambda = 1.0$. The data points forming these distributions are from Liu & Wang (2020).

Kremer et al. (2017) recently argued that about 2700 double WDs will be detected by space-based GW detectors like LISA. For more studies about the GW signals from double WDs, see, e.g, Liu (2009), Yu & Jeffery (2010, 2015), Liu et al. (2012), Liu & Zhang (2014), Zou et al. (2020), etc.

The chirp mass is a mass function of double WDs that can be measured by the GW detectors directly. Figure 13 depicts the chirp mass distributions of different kinds of double WDs for producing AIC events at the moment of their birth, which mainly ranges from 0.55 to $1.25\,M_\odot$. For the case of double CO WDs, their chirp masses are in the range of $0.55-1.05\,M_\odot$ and there are two peaks at $0.75\,M_\odot$ and $0.95\,M_\odot$, in which the origin of the double peaks is similar to that of Figure 12. The chirp masses of ONe WD+CO WD systems are in the range of $0.55-1.2\,M_\odot$ and have a peak at $0.85\,M_\odot$, whereas the chirp masses of double ONe WDs range from 0.8 to $1.25\,M_\odot$ and have a peak at $1.1\,M_\odot$.

The GW strain amplitude (h) is defined as the fractional change in separation once a GW passes through the detectors. Figure 14 presents the dimensionless h distributions of different kinds of double WDs for producing AIC events in the $\log h - \log f_{\rm GW}$ plane, in which the GW frequency of double WDs $f_{\rm GW} = 2/P_{\rm orb}$ where $P_{\rm orb}$ is the orbital period of double WDs at the moment of their formation. Like previous studies in Ruiter et al. (2019), we simply assume that the distance d from double WDs to the detectors is 8.5 kpc which is an appropriate distance from our solar system to the Galactic center. In reality, the distance from double WDs to the detectors should have a wider distribution in the Galaxy but not simply set to be 8.5 kpc.

The GW strain amplitude h in Figure 14 ranges from $10^{-24}-10^{-21}$ and $f_{\rm GW}$ is in the range of $10^{-5}-10^{-1}$ Hz. For different kinds of double WDs, there are two parts for the dimensionless h distributions, in which the right small part originates from Scenario C and the left part mainly originates from Scenarios A and B in Figures 9–10 (for the double CO WDs, see fig. 11 of Wang 2018b). Furthermore, the h and $f_{\rm GW}$ for double ONe WDs is larger than that of ONe WD+CO WD systems, and the h and $f_{\rm GW}$ for ONe WD+CO WD systems tend to be larger than those of double CO WDs. We estimate that more than half of double WDs for producing AIC events are capable of being observed by future space-based GW detectors, such as LISA, TianQin, Taiji, etc.

5 DETECTION OF AIC EVENTS

Identification of AIC events is challenging. Up to now, there is still no exclusively direct evidence for AIC events in observations. Some possible reasons are summarized as below: (1) AIC events are expected to be relatively faint optical transients, which are fainter than a typical normal SNe Ia by 5 mag or more and last for only a few days to a week, indicating that this kind of object is difficult to be discovered. (2) AIC events with low luminosities may have been already observed by some ongoing surveys, but they were mixed with some other (optically) faint transients, such as rapidly declining SN-like transients, fast-rising blue optical transients, kilonovae, fast radio bursts, gamma-ray bursts, etc. (3) The predicted ejecta mass and ^{56}Ni synthesized during the collapse are still not well determined. Another weakness for the AIC scenario is that it is difficult to reproduce the surface B-field and the spin rate of the observed NSs that may be associated with AIC (see Tauris et al. 2013). The AIC scenario results in the production of normal NSs that then continue to accrete material, leading to a weaker B-field and a faster spin. This is contrary to the observed NSs (characterized by relatively high B-fields and slow spin) that are potential candidates for having formed through AIC in globular clusters or in the Galactic disk (see table 1 of Tauris et al. 2013).

For the single-degenerate model, dense circumstellar matter may be formed around the pre-AIC systems. The ejecta from the AIC collides with the dense circumstellar matter, probably forming a strong shock. The strong shock can produce synchrotron emission that may be detected in radio frequencies. Piro & Thompson (2014) suggested that strong radio emission would happen for an AIC event that originates from the evolution of ONe WD+RG systems. They claimed that the ejecta of the AIC will collide with the surface of the RG star, producing strong X-ray emission lasting for $\sim$1 hr followed by an optical signal from the shocked region, although the signal is strongly depen-

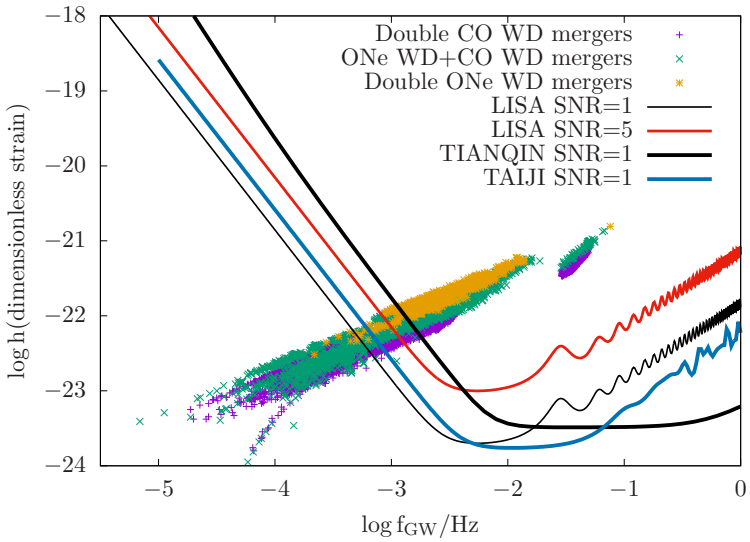

Fig. 14 Dimensionless GW strain amplitude of different kinds of double WDs for producing AIC events with $\alpha_{\rm CE}\lambda = 1.0$, in which we simply set the distance from double WDs to the detectors as 8.5 kpc. The sensitivity curves for the future space-based GW observatory LISA are based on Larson and Hiscock & Hellings: `http://www.srl.caltech.edu/~shane/sensitivity`. The sensitivity curve for TianQin is from Wang et al. (2019). The sensitivity curve for Taiji is from Ruan et al. (2020b). The data points forming these distributions are from Liu & Wang (2020).

dent on the viewing angle. Moriya (2016) suggested that AIC events may act as radio bright but optically faint transients, likely leading to strong X-ray emission owing to the interaction between AIC ejecta and dense circumstellar matter in single-degenerate systems. The radio signals of AIC are expected to be detected by radio transient surveys such as the Very Large Array Sky Survey and Square Kilometre Array transient survey (e.g., Moriya 2016).

For the double-degenerate model, it is not expected to have dense circumstellar matter before AIC, thus no strong radio emission is predicted in the single-degenerate model. As shown in Figure 12, the merging of double WDs can form supermassive ($>2.2\,M_{\odot}$) NSs that require rapid rotation to support themselves (e.g., Metzger et al. 2015). These supermassive NSs may lose their rotational energy immediately through r-mode instability and finally collapse into black holes. It has been suggested that the collapsing of supermassive NSs may produce fast radio bursts if they are strongly magnetized (e.g., Moriya 2016). Lyutikov & Toonen (2017) proposed an alternative way to form prompt short gamma-ray bursts following the merging of ONe WD+CO WD. Rueda et al. (2019) predicted that the primary WD during the post-merger time may appear as a pulsar, depending on the rotation period and the value of magnetic fields. In addition, Yu et al. (2019a) recently suggested that searching for dust-affected optical transients and shock-driven radio transients will help to unveil the nature and evolution of double WD mergers with super-$M_{\rm Ch}$.

Anderson et al. (2019) reported a radio transient, VTC J095517.5+690813, that became bright in the radio but without an optical counterpart in the observations. By comparing the predicted radio emission from an AIC with that from VTC J095517.5+690813, Moriya (2019) recently suggested that the radio transient can be reasonably explained by AIC of a WD. In addition, Scholz et al. (2016) discovered a persistent radio source associated with fast radio burst FRB 121102. The persistent radio source has been thought to be produced by a weak stellar explosion with a small ejected mass that may be consistent with the AIC scenario, whereas the resulting NS acts as the energy source of FRB 121102 (e.g., Waxman 2017; Sharon & Kushnir 2020). Margalit et al. (2019) recently also associated the progenitor of FRB 121102 with AIC. Therefore, there is a possibility that AIC events might be first discovered as fast radio bursts, and then followed by optically faint but radio bright transients (e.g., Moriya 2019). Additionally, Moriya (2019) recently speculated that it is possible to distinguish the single-degenerate model and the double-degenerate models via radio light curves once an AIC event has been identified.

AT2018cow was discovered by the Asteroid Terrestrial-impact Last Alert System (ATLAS; see Tonry et al. 2018). It is likely to be the brightest member of the class of fast-rising blue optical transients (e.g., Prentice et al. 2018; Margutti et al. 2019). Yu et al. (2015) associated the AIC scenario with the recently discovered fast-evolving luminous transients. In a further work, Yu et al. (2019b) predicted hard and soft X-ray emissions

from the AIC of WDs, providing a clear observational feature for identifying AIC events in future observations, especially for AT2018cow. Lyutikov & Toonen (2019) recently argued that the fast-rising blue optical transients and its brightest member AT2018cow may result from the merging of an ONe WD with another WD. Note that Soker et al. (2019) proposed a CE jets SN scenario for the formation of AT2018cow, in which a jet driven by an accreting NS collides with a giant star. Note also that the unusual transient AT2018cow was claimed as a WD tidal disruption event (see Kuin et al. 2019).

Furthermore, faint rapidly declining SN-like transients are possible candidates of AIC events. Apart from the most detailed observed kilonova AT2017gfo, McBrien et al. (2019) recently suggested that SN 2018kzr is the second fastest declining SN-like transient known so far, which was independently discovered by the Zwicky Transient Facility (ZTF; see Bellm et al. 2019) and the ATLAS survey (see Tonry et al. 2018). By modeling the bolometric light curves and early spectra, McBrien et al. (2019) estimated that SN 2018kzr has a low ejecta mass composed of intermediate mass elements, disfavoring the merging of double NSs. Thus, they argued that AIC of an ONe WD may provide an alternative explanation for the formation of the rapidly declining transient.

6 SUMMARY

The AIC scenario has been proposed as a theoretically predicted outcome of ONe WDs when they grow in mass close to $M_{\rm Ch}$, relating to the formation of NS systems. So far, there has been no direct detection of any AIC event, likely because this kind of event is a relatively faint optical transient and short-lived. Currently, the most studied evolutionary pathways for AIC events are the single-degenerate model and the double-degenerate model. We review recent progress on the two classic progenitor models of AIC events. We also review recent results on binary population synthesis and summarize recent theoretical and observational constraints on the detection of AIC events.

In the single-degenerate model, pre-AIC systems could potentially be identified as supersoft X-ray sources, symbiotics and cataclysmic variables. Post-AIC systems in the single-degenerate model may evolve to some different kinds in NS systems if AIC happens, mainly depending on the chemical components of the mass donors, as follows: (1) The post-AIC systems with MS donors are likely to be identified as LMXBs and the resulting fully recycled MSPs with He WD companions. (2) The post-AIC systems with RG donors could form LMXBs and the more mildly recycled MSPs with He/CO WD companions, especially for MSPs with much longer orbital periods compared with MS donors. (3) The post-AIC systems with He star donors could potentially be identified as IMXBs and eventually produce IMBPs with short orbital periods.

In the double-degenerate model, pre-AIC systems are close double WDs with short orbital periods. The double WDs for producing AIC events are capable of being observed by future space-based GW detectors, such as LISA, TianQin, Taiji, etc. Post-AIC systems in the classic double-degenerate model are single isolated NSs that may correspond to a specific kind of NS and display some peculiar properties compared with those from core-collapse SNe.

AIC events are likely to be radio bright but optically faint. In order to provide constraints on the progenitor models of AIC events, large samples of WD binaries are required in the observations. Meanwhile, identifying AIC events in future transient surveys and understanding their electromagnetic signals are important for confirmation of the AIC process. More theoretical and observational investigations would be helpful for our understanding of this type of event. Future observational surveys are expected to finally confirm such events with low luminosities and to clarify the long-term issue that the current stellar evolution theories confront.

Acknowledgements We acknowledge the referee for valuable comments that helped us to improve this review. We also thank Noam Soker, Wencong Chen, Takashi Moriya, Xiangcun Meng, Matthias U. Kruckow, Iminhaji Ablimit, Zongkuan Guo, Hailiang Chen, Jujia Zhang, Yiming Hu, Haijun Tian, Yan Gao and Wenshi Tang for their helpful discussions and suggestions. BW is supported by the National Natural Science Foundation of China (Grant Nos. 11521303, 11673059 and 11873085), the Chinese Academy of Sciences (No. QYZDB-SSW-SYS001) and Yunnan Province (Nos. 2018FB005 and 2019FJ001). DL is supported by the National Natural Science Foundation of China (Grant No. 11903075) and the Western Light Youth Project of Chinese Academy of Sciences.

References

Abbott, B. P., Abbott, R., Abbott, T. D., et al. 2016, Phys Rev Lett, 116, 061102
Abbott, B. P., Abbott, R., Abbott, T. D., et al. 2017a, ApJ, 851, L35
Abbott, B. P., Abbott, R., Abbott T. D., et al. 2017b, Phys Rev Lett, 119, 141101
Abdikamalov, E. B., Ott, C. D., Rezzolla, L., et al. 2010, Phys. Rev. D, 81, 044012
Ablimit, I. 2019, ApJ, 881, 72
Ablimit, I., & Li, X.-D. 2015, ApJ, 800, 98
Ablimit, I. & Maeda, K. 2019a, ApJ, 871, 31
Ablimit, I. & Maeda, K. 2019b, ApJ, 885, 99

Ablimit, I., Xu, X.-J., & Li, X.-D. 2014, ApJ, 780, 80
Anderson, G. E., Miller-Jones, J. C. A., Middleton, M. J., et al. 2019, MNRAS, 489, 1181
Andrea, J., Drechsel, H., & Starrfield, S. 1994, A&A, 291, 869
Antoniadis, J., Freire, P. C. C., Wex, N., et al. 2013, Science, 340, 448
Ashok, N. M., & Banerjee, D. P. K. 2003, A&A, 409, 1007
Badenes, C., Mullally, F., Thompson, S. E., & Lupton, R. H. 2009, ApJ, 707, 971
Bailyn, C. D., & Grindlay, J. E. 1990, ApJ, 353, 159
Bao, J., Shi, C., Wang, H., et al. 2019, Phys. Rev. D, 100, 084024
Belczyński, K., & Mikołajewska, J. 1998, MNRAS, 296, 77
Belczyński, K., Askar, A., Arca-Sedda, M., et al. 2018, A&A, 615, A91
Bellm, E. C., Kulkarni, S. R., Graham, M. J., et al. 2019, PASP, 131, 018002
Belloni, D., Mikołajewska, J., Iłkiewicz, K., et al. 2020, submitted to MNRAS (arXiv:2004.05453)
Beznogov, M. V., Page, D., & Ramirez-Ruiz, E. 2020, ApJ, 888, 97
Bhattacharya, D., & van den Heuvel, E. P. J. 1991, Phys. Rep., 203, 1
Bisscheroux, B. C., Pols, O. R., Kahabka, P., & van den Heuvel, E. P. J. 1997, A&A, 317, 815
Borges, S. V., Rodrigues, C. V., Coelho, J. G., et al. 2020, ApJ, 895, 26
Boyles, J., Lorimer, D. R., Turk, P. J., et al. 2011, ApJ, 742, 51
Brandi, E., Quiroga, C., Mikołajewska, J., et al. 2009, A&A, 497, 815
Brooks, J., Bildsten, L., Schwab, J., & Paxton, B. 2016, ApJ, 821, 28
Brooks, J., Schwab, J., Bildsten, L., Quataert, E., & Paxton, B. 2017, ApJ, 843, 151
Bulla, M., Sim, S. A., Pakmor, R., et al. 2016, MNRAS, 455, 1060
Cao, X.-F., Yu, Y.-W., & Zhou, X. 2018, ApJ, 858, 89
Camisassa, M. E., Althaus, L. G., Córsico, A., et al. 2019, A&A, 625, A87
Canals, P., Torres, S., & Soker, N. 2018, MNRAS, 480, 4519
Canal, R., Garcia, D., Isern, J., & Labay, J. 1990a, ApJ, 356, L51
Canal, R., Isern, J., & Labay, J. 1990b, ARA&A, 28, 183
Carrasco, J. M., Catalń, S., Jordi, C., et al. 2014, A&A, 565, A11
Casanova, J., José, J., GarcJosía-Berro, E., & Shore, S. N. 2016, A&A 595, A28
Chanmugam, G., & Brecher, K. 1987, Nature, 329, 696
Chen, H.-L., Chen, X., Tauris, T. M., et al. 2013, ApJ, 775, 27
Chen, M. C., Herwig, F., Denissenkov, P. A., & Paxton, B. 2014, MNRAS, 440, 1274
Chen, W.-C., Liu, D., & Wang, B. 2020, ApJL, 900, L8
Chen, W.-C., & Liu, W.-M. 2013, MNRAS, 432, L75
Chen, W.-C., Liu, X.-W., Xu, R.-X., & Li, X.-D. 2011, MNRAS, 410, 1441
Chen, W.-C., Li, X.-D., & Xu, R.-X. 2011, A&A, 530, A104
Chen, X., Han, Z., & Tout, C. A. 2011, ApJ, 735, L31
Chen, X., Jeffery, C. S., Zhang, X., & Han, Z. 2012, ApJL, 755, L9
Crocker, R. M., Ruiter, A. J., Seitenzahl, I. R., et al. 2017, Nature Astronomy, 1, 0135
Cromartie, H. T., Fonseca, E., Ransom, S. M., et al. 2020, Nature Astronomy, 4, 72
Dan, M., Rosswog, S., Guillochon, J., & Ramirez-Ruiz, E. 2012, MNRAS, 422, 2417
Dar, A., Kozlovsky, B. Z., Nussinov, S., & Ramaty, R. 1992, ApJ, 388, 164
Darbha, S., Metzger, B. D., Quataert, E., et al. 2010, MNRAS, 409, 846
Demorest, P. B., Pennucci, T., Ransom, S. M., et al. 2010, Nature, 467, 1081
Denissenkov, P. A., Herwig, F., Bildsten, L., & Paxton, B. 2013, ApJ, 762, 8
Denissenkov, P. A., Truran, J. W., Pignatari M., et al. 2014, MNRAS, 442, 2058
Dessart, L., Burrows, A., Livne, E., & Ott, C. D. 2007, ApJ, 669, 585
Dessart, L., Burrows, A., Ott, C. D., et al. 2006, ApJ, 644, 1063
Doherty, C. L., Gil-Pons, P., Siess, L., & Lattanzio, J. C. 2017, PASA, 34, 56
Downen, L. N., Iliadis, C., José, J., & Starrfield, S. 2013, ApJ, 762, 105
Drake, J. J., Delgado, L., Laming, J. M., et al. 2016, ApJ, 825, 95
Eggleton, P. P. 2006, Evolutionary Processes in Binary and Multiple Stars (Cambridge: Cambridge Univ. Press)
Evans, C. R., Iben, I. Jr., & Smarr, L. 1987, ApJ, 323, 129
Feng, W., Wang, H., Hu, X., Hu, Y., & Wang, Y. 2019, Phys. Rev. D, 99, 123002
Fesen, R. A., Höflich, P. A., & Hamilton, A. J. S. 2015, ApJ, 804, 140
Fontaine, G., Brassard, P., & Bergeron, P. 2001, PASP, 113, 409
Freire, P. C. C., & Tauris, T. M. 2014, MNRAS, 438, L86
Fryer, C., Benz, W., Herant, M., & Colgate, S. A. 1999, ApJ, 516, 892
Ge, H., Hjellming, M. S., Webbink, R. F., et al. 2010, ApJ, 717, 724
Gehrz, R. D., Truran, J. W., Williams, R. E., & Starrfield, S. 1998, PASP, 110, 3
Geier, S., Heber, U., Kupfer, T., & Napiwotzki, R. 2010, A&A, 515, A37
Geier, S., Nesslinger, S., Heber, U., et al. 2007, A&A, 464, 299
Genest-Beaulieu, C., & Bergeron, P. 2019, ApJ, 882, 106
Gil-Pons, P., & García-Berro, E. 2001, A&A, 375, 87
Gil-Pons, P., García-Berro, E. , José, J., et al. 2003, A&A 407, 1021
Glasner, S. A., Livne, E., & Truran, J. W. 2012, MNRAS, 427, 2411
Hachisu, I., Kato, M., Kato, T., et al. 2000, ApJ, 528, L97
Hachisu, I., Kato, M., & Nomoto, K. 1996, ApJ, 470, L97

Hachisu, I., Kato, M., Nomoto, K., & Umeda, H. 1999a, ApJ, 519, 314
Hachisu, I., Kato, M., & Nomoto, K., 1999b, ApJ, 522, 487
Han, Z. 1998, MNRAS, 296, 1019
Han, Z., & Podsiadlowski, Ph. 2004, MNRAS, 350, 1301
Han, Z., & Podsiadlowski, Ph. 2006, MNRAS, 368, 1095
Han, Z., Podsiadlowski, Ph., & Eggleton, P. P. 1994, MNRAS, 270, 121
Han, Z., Podsiadlowski, Ph., & Eggleton, P. P. 1995, MNRAS, 272, 800
Han, Z., Podsiadlowski, Ph., Maxted, P. F. L., & Marsh, T. R. 2003, MNRAS, 341, 669
Han, Z., & Webbink, R. F. 1999, A&A, 349, L17
Hollands, M. A., Tremblay, P.-E. , Gänsicke, B. T., et al. 2020, Nature Astronomy, in press (arXiv:2003.00028)
Hoyle, F., & Fowler, W. A. 1960, ApJ, 132, 565
Hurley, J. R., Tout, C. A., Wickramasinghe, D. T., et al. 2010, MNRAS, 402, 1437
Iben, I., & Tutukov, A. V. 1984, ApJS, 54, 335
Iben, I., & Tutukov, A. V. 1985, ApJS, 58, 661
Isern, J., Canal, R., & Labay, J. 1991, ApJ, 372, L83
Ivanova, N., Heinke, C. O., Rasio, F. A., et al. 2008, MNRAS, 386, 553
Ivanova, N., Justham, S., Avendano Nandez, J. L., & Lombardi, J. C. 2013, Science, 339, 433
Ivanova, N., & Taam, R. E. 2004, ApJ, 601, 1058
Jia, K., & Li, X.-D. 2014, ApJ, 791, 127
Jiang, L., Wang, N., Chen, W.-C., et al. 2020, A&A, 633, A45
Justham, S., Rappaport, S., & Podsiadlowski, P. 2006, MNRAS, 366, 1415
Jones, S., Röpke, F. K., Pakmor, R., et al. 2016, A&A, 593, A72
Kahabka, P., & van den Heuvel, E. P. J. 1997, ARA&A, 35, 69
Kalita, S., Mukhopadhyay, B., Mondal, T., & Bulik, T. 2020, ApJ, 896, 69
Kashyap, R., Haque, T., Lorén-Aguilar, P., et al. 2018, ApJ, 869, 140
Kato, M., Hachisu, I., Kiyota, S., & Saio, H. 2008, ApJ, 684, 1366
Kawka, A., Briggs, G. P., Vennes, S., et al. 2017, MNRAS, 466, 1127
Kitaura, F. S., Janka, H.-T., & Hillebrandt, W. 2006, A&A, 450, 345
Koester, D., Napiwotzki, R., Christlieb, N., et al. 2001, A&A, 378, 556
Kozai, Y. 1962, AJ, 67, 591
Kremer, K., Breivik, K., Larson, S. L., et al. 2017, ApJ, 846, 95
Kromer, M., Pakmor, R., Taubenberger, S., et al. 2013, ApJL, 778, L18
Krtička, J., Janík, J., Krtičková, I., et al. 2019, A&A, 631, A75
Kuin, N. P. M., Wu, K., Oates, S., et al. 2019, MNRAS, 487, 2505
Kulkarni, S. R., & Narayan, R. 1988, ApJ, 335, 755
Langer, N., Deutschmann, A., Wellstein, S., & Höflich, P. 2000, A&A, 362, 1046
Li, X.-D. 2002, ApJ, 564, 930
Li, X.-D. 2015, New Astron. Rev., 64, 1
Li, X.-D., & van den Heuvel, E. P. J. 1997, A&A, 322, L9
Li, X.-D., & Wang, Z.-R. 1998, ApJ, 500, 935
Lidov, M. L. 1962, Planet. Space Sci., 9, 719
Liu, B.-S., & Li, X.-D. 2019, RAA (Research in Astronomy and Astrophysics), 19, 044
Liu, D., & Wang, B. 2020, MNRAS, 494, 3422
Liu, D., Wang, B., Chen, W., Zuo, Z., & Han, Z. 2018a, MNRAS, 477, 384
Liu, D., Wang, B., & Han, Z. 2018b, MNRAS, 473, 5352
Liu, D., Wang, B., Ge, H., Chen, X., & Han, Z. 2019, A&A, 622, A35
Liu, D., Wang, B., Podsiadlowski, Ph., & Han, Z. 2016, MNRAS, 461, 3653
Liu, D., Wang, B., Wu, C., & Han, Z. 2017, A&A, 606, A136
Liu, D., Zhou, W., Wu, C., & Wang, B. 2015, RAA (Research in Astronomy and Astrophysics), 15, 1813
Liu, J. 2009, MNRAS, 400, 1850
Liu, J., & Zhang, Y. 2014, PASP, 126, 211
Liu, J., Zhang, Y., Zhang, H., Sun, Y., & Wang, N. 2012, A&A, 540, A67
Liu, W.-M., & Chen, W.-C. 2014, MNRAS, 441, 3615
Liu, W.-M., & Li, X.-D. 2017, ApJ, 851, 58
Lorimer, D. R. 2008, LRR, 11, 8
Luo, J., Chen, L. S., Duan, H. Z., et al. 2016, Class Quantum Grav, 33, 035010
Luo, Z., Guo, Z., Jin, G., et al. 2020, Results in Physics, 16, 102918
Lü, G., Zhu, C., Wang, Z., & Wang, N. 2009, MNRAS 396, 1086
Lyutikov, M., & Toonen, S. 2017, in preprint (arXiv:1709.02221)
Lyutikov, M., & Toonen, S. 2019, MNRAS 487, 5618
Margalit, B., Berger, E., & Metzger, B. D. 2019, ApJ, 886, 110
Margutti, R., Metzger, B. D., Chornock, R., et al. 2019, ApJ, 872, 18
Marquardt, K. S., Sim, S. A., Ruiter, A. J., et al. 2015, A&A, 580, A118
Marsh, T. R. 2011, Class Quantum Grav, 28, 094019
Mason, E. 2011, A&A, 532, L11
Mason, E. 2013, A&A, 556, C2
Maxted, P. F. L., Marsh, T. R., & North, R. C. 2000, MNRAS, 317, L41
McBrien O. R., Smartt S. J., Chen T. W. et al., 2019, ApJL, 885, L23
Meng, X., Chen, X., & Han, Z. 2009, MNRAS, 395, 2103
Meng, X., & Han, Z. 2015, A&A, 573, A57
Mereghetti, S., Tiengo, A., Esposito, P., et al. 2009, Science, 325, 1222
Mereghetti, S., Pintore, F., Esposito, P., et al. 2016, MNRAS, 458, 3523
Metzger, B. D., Margalit, B., Kasen, D., & Quataert, E. 2015, MNRAS, 454, 3311

Metzger, B. D., Piro, A. L., & Quataert, E. 2009, MNRAS, 396, 1659
Mikołajewska, J., & Shara, M. M. 2017, ApJ, 847, 99
Miyaji, S., Nomoto, K., Yokoi, K., & Sugimoto, D. 1980, PASJ, 32, 303
Moll, R., Raskin, C., Kasen, D., & Woosley, S. E. 2014, ApJ, 785, 105
Moriya, T. J. 2016, ApJL, 830, L38
Moriya, T. J. 2019, MNRAS, 490, 1166
Naoz, S. 2016, ARA&A, 54, 441
Napiwotzki, R., Karl, C.A., Nelemans, G., et al. 2007, ASPC, 372, 387
Napiwotzki, R., Yungelson, L., Nelemans, G., et al. 2004, ASPC, 318, 402
Nelemans, G. 2013, in ASP Conf. Ser. 467, 9th LISA Symposium. Astron. Soc. Pac., San Francisco, eds. Auger, G., Binétruy, P., & Plagnol, E. 27
Nelemans, G., & Jonker, P. G. 2010, New Astro. Rev., 54, 87
Nelemans, G., Napiwotzki, R., Karl, C., et al. 2005, A&A, 440, 1087
Nelemans, G., Yungelson, L. R., Portegies Zwart, S. F., & Verbunt, F. 2001a, A&A, 365, 491
Nelemans, G., Portegies Zwart, S. F., Verbunt, F., & Yungelson, L. R. 2001b, A&A, 368, 939
Nelemans, G., Yungelson, L. R., & Portegies Zwart, S. F. 2004, MNRAS, 349, 181
Nelson, L. A., Rappaport, S. A., & Joss, P. C. 1986, ApJ, 304, 231
Nomoto, K., & Iben, I. 1985, ApJ, 297, 531
Nomoto, K., & Kondo, Y. 1991, ApJ, 367, L19
Nomoto, K., Miyaji, S., Sugimoto, D., & Yokoi, K. 1979, in IAU Coll., White Dwarfs and Variable Degenerate Stars, eds. H. M. van Horn, & V. Weidemann, 53, 56
Nomoto, K., Thielemann, F-K., & Yokoi, K. 1984, ApJ, 286, 644
Orlando, S., Drake, J. J., & Miceli, M. 2017, MNRAS, 464, 5003
Ostriker, J. P., & Bodenheimer, P. 1968, ApJ, 151, 1089
Paczyński, B. 1970, Acta Astron., 20, 47
Pakmor, R., Hachinger, S., Röpke, F. K., & Hillebrandt, W. 2011, A&A, 528, A117
Pakmor, R., Kromer, M., Röpke, F. K., et al. 2010, Nature, 463, 61
Parsons, S. G., Brown, A. J., Littlefair, S. P., et al. 2020, Nature Astronomy, in press (arXiv:2003.07371)
Perets, H. B., Gal-Yam, A., Mazzali, P. A., et al. 2010, Nature, 465, 322
Piro, A. L., & Kulkarni, S. R. 2013, ApJ, 762, L17
Piro, A. L., & Kollmeier, J. A. 2016, ApJ, 826, 97
Piro, A. L., & Thompson, T. A. 2014, ApJ, 794, 28
Podsiadlowski, P. 2010, Astron. Nachr., 331, 218
Podsiadlowski, P., Rappaport, S., & Pfahl, E. D. 2002, ApJ, 565, 1107
Popov, S. B. 2011, preprint (arXiv:1111.1158)
Popov, S. B., Mereghetti, S., Blinnikov, S. I., et al. 2018, MNRAS, 474, 2750
Prentice, S. J., Maguire, K., Smartt, S. J., et al., 2018, ApJL, 865, L3
Qian, Y.-Z., & Wasserburg, G. J. 2007, Phys. Rep., 442, 237
Rappaport, S., Di Stefano, R., & Smith, J. D. 1994, ApJ, 426, 692
Rodríguez-Gil, P., Santander-García, M., Knigge, C., et al. 2010, MNRAS, 407, L21
Ruan, W.-H., Liu, C., Guo, Z.-K., Wu, Y.-L., & Cai, R.-G. 2019, preprint (arXiv:1909.07104)
Ruan, W.-H., Guo, Z.-K., Cai, R.-G., & Zhang, Y.-Z. 2020a, Int. J. Mod. Phys., 35, 2050075
Ruan, W.-H., Liu, C., Guo, Z.-K., Wu, Y.-L., & Cai, R.-G. 2020b, Nature Astronomy, 4, 108
Rueda, J. A., Ruffini, R., Wang, Y., et al. 2019, JCAP, 03, 044
Ruiter, A. J., Belczynski, K., Benacquista, M., et al. 2010, ApJ, 717, 1006
Ruiter, A. J., Belczynski, K., & Fryer, C. L. 2009, ApJ, 699, 2026
Ruiter, A. J., Sim, S. A., Pakmor, R., et al. 2013, MNRAS, 429, 1425
Ruiter, A. J., Ferrario, L., Belczynski, K., et al. 2019, MNRAS, 484, 698
Sabach, E., & Soker, N. 2014, MNRAS, 439, 954
Saio, H., & Jeffery, C. S. 2000, MNRAS, 313, 671
Saio, H., & Jeffery, C. S. 2002, MNRAS, 333, 121
Saio, H., & Nomoto, K. 1985, A&A, 150, L21
Saio, H., & Nomoto, K. 1998, ApJ, 500, 388
Santander-García, M., Rodríguez-Gil, P., Corradi, R. L. M., et al. 2015, nature, 519, 63
Sato, Y., Nakasato, N., Tanikawa, A., Nomoto, K., Maeda, K., & Hachisu, I. 2016, ApJ, 821, 67
Scholz, P., Spitler, L., Hessels, J., et al. 2016, ApJ, 833, 177
Schwab, J., & Rocha, K. A. 2019, ApJ, 872, 131
Schwab, J., Quataert, E., & Bildsten, L. 2015, MNRAS, 453, 1910
Schwab, J., Quataert, E., & Kasen, D. 2016, MNRAS, 463, 3461
Shao, Y. & Li, X.-D. 2012, ApJ, 756, 85
Sharon, A., & Kushnir, D. 2020, ApJ, 894, 146
Shi, C., Bao, J., Wang, H., et al. 2019, Phys. Rev. D, 100, 044036
Shore, S. N., De Gennaro Aquino, I., Schwarz, G. J., et al. 2013, A&A, 553, A123
Shore, S. N., Schwarz, G., Bond, H. E., et al. 2003, AJ, 125, 1507
Smedley, S. L., Tout, C. A., Ferrario, L., & Wickramasinghe, D. T. 2017, MNRAS, 464, 237
Soker, N. 2019, Science China Physics, Mechanics, and Astronomy, 62, 119501
Soker, N. 2020, RAA (Res. Astron. Astrophys.), 20, 024
Soker, N., Grichener, A., & Gilkis, A. 2019, MNRAS, 484, 4972
Taam, R. E., & van den Heuvel, E. P. J. 1986, ApJ, 305, 235
Tang, S., Grindlay, J., Moe, M., et al. 2012, ApJ, 751, 99
Tang, W., Liu, D., & Wang, B. 2019, MNRAS, 490, 752
Tanikawa, A., Nakasato, N., Sato, Y., et al. 2015, ApJ, 807, 40

Taubenberger, S., Kromer, M., Pakmor, R., et al. 2013, ApJ, 775, L43
Tauris, T. M. 2018, PhRvL, 121, 131105
Tauris, T. M., Langer, N., & Kramer, M. 2012, MNRAS, 425, 1601
Tauris, T. M., Sanyal, D., Yoon, S.-C., & Langer, N. 2013, A&A, 558, A39
Tauris, T. M., & van den Heuvel, E. P. J. 2006, in Compact Stellar X-ray Sources, eds. W. Lewin & M. van der Klis (Cambridge: Cambridge Univ. Press), 623
Tauris, T. M., van den Heuvel, E. P. J., & Savonije, G. J. 2000, ApJ, 530, L93
Thackeray, A. D. 1970, MNRAS, 150, 215
Thoroughgood, T. D., Dhillon, V. S., Littlefair, S. P., et al. 2001, MNRAS, 327, 1323
Tian, H.-J., El-Badry, K., Rix, H.-W., et al. 2020a, ApJS, 246, 4
Tian, H.-J., Xu, Y., Liu, C., et al. 2020b, ApJS, 248, 28
Tian, H.-J., Gupta, P., Sesar, B., et al. 2017, ApJS, 232, 4
Timmes, F. X., Woosley, S. E., & Taam, R. E. 1994, ApJ, 420, 348
Tonry, J. L., Denneau, L., Heinze, A. N., et al. 2018, PASP, 130, 064505
Toonen, S., Hollands, M., Gänsicke, B. T., & Boekholt, T. 2017, A&A, 602, A16
Toonen, S., Nelemans, G., & Portegies, Z. S. 2012, A&A, 546, A70
Tovmassian, G., Yungelson, L., Rauch, T., et al. 2010, ApJ, 714, 178
Truran, J. W., & Cameron, A. G. W. 1971, Astrophys. Space. Sci., 14, 179
Usov, V. V. 1992, Nature, 357, 472
van den Heuvel, E. P. J. 1984, J. Astrophys. Astron., 5, 209
van den Heuvel, E. P. J. 2009, in Astrophysics and Space Science Library, 359, Physics of Relativistic Objects in Compact Binaries: From Birth to Coalescence, eds. Colpi, M., Casella, P., Gorini, V., Moschella, U., & Possenti, A. (Berlin: Springer-Verlag), 125
van den Heuvel, E. P. J., Bhattacharya, D., Nomoto, K., & Rappaport, S. A. 1992, A&A, 262, 97
van Paradijs, J., van den Heuvel, E. P. J., Kouveliotou, C., et al. 1997, A&A, 317, L9
Verbunt, F., & Freire, P. C. C. 2014, A&A, 561, A11
Wanajo, S., Hashimoto, M.-A., & Nomoto, K. 1999, ApJ, 523, 409
Wang, B. 2018a, MNRAS, 481, 439
Wang, B. 2018b, RAA (Research in Astronomy and Astrophysics), 18, 049
Wang, B., Meng, X., Chen, X., et al. 2009, MNRAS, 395, 847
Wang, B., & Han, Z. 2010, A&A, 515, A88
Wang, B., & Han, Z. 2012, New Astron. Rev., 56, 122
Wang, B., Justham, S., Liu, Z., et al. 2014, MNRAS, 445, 2340
Wang, B., Li, X.-D., & Han, Z. 2010, MNRAS, 401, 2729
Wang, B., Podsiadlowski, Ph., & Han, Z. 2017, MNRAS, 472, 1593
Wang, H.-T., Jiang, Z., Sesana, A., et al. 2019, Phys. Rev. D, 100, 043003
Warner, B. 1995, Cataclysmic Variable Stars (Cambridge: Cambridge University Press)
Waxman, E. 2017, ApJ, 842, 34
Webbink, R. F. 1984, ApJ, 277, 355
Wheeler, J. C., Cowan, J. J., & Hillebrandt, W. 1998, ApJ, 493, L101
Woods, T. E., & Ivanova, N. 2011, ApJL, 739, L48
Woosley, S. E., & Baron, E. 1992, ApJ, 391, 228
Woudt, P. A., & Steeghs, D. 2005, ASPC, 330, 451
Woudt, P. A., Steeghs, D., Karovska, M., et al. 2009, ApJ, 706, 738
Wu, C., & Wang, B. 2018, RAA (Research in Astronomy and Astrophysics), 18, 36
Wu, C., & Wang, B. 2019, MNRAS, 486, 2977
Wu, C., Wang, B., & Liu, D. 2019, MNRAS, 483, 263
Wu, C., Wang, B., Liu, D., & Han, Z. 2017, A&A, 604, A31
Wu, C., Wang, B., Wang, X., Maeda, K., & Mazzali, P. 2020, MNRAS, 495, 1445
Xiao, D., Mészáros, P., Murase, K., & Dai, Z. 2016, ApJ, 832, 20
Xu, X.-J., & Li, X.-D. 2009, A&A, 495, 243
Yoon, S.-C., & Langer, N. 2004, A&A, 419, 623
Yoon, S.-C., & Langer, N. 2005, A&A, 435, 967
Yoon, S.-C., Podsiadlowski, P., & Rosswog, S. 2007, MNRAS, 380, 933
Yu, S., & Jeffery, C. S. 2010, A&A, 521, A85
Yu, S., & Jeffery, C. S. 2015, MNRAS, 448, 1078
Yu, Y.-W., Li, S.-Z., & Dai, Z.-G. 2015, ApJL, 806, L6
Yu, Y.-W., Chen, A., & Wang, B. 2019a, ApJL, 870, L23
Yu, Y.-W., Chen, A., & Li, X.-D. 2019b, ApJL, 877, L21
Yungelson, L. R., & Kuranov, A. G. 2017, MNRAS, 464, 1607
Yungelson, L. R., & Livio, M. 1998, ApJ, 497, 168
Zhang, X.-F., & Jeffery, C. S. 2012, MNRAS, 419, 452
Zhang, X.-F., Jeffery, C. S., Chen, X., & Han, Z. 2014, MNRAS, 445, 660
Zhang, X.-F., Liu, J.-Z., Jeffery, C. S., et al. 2018, RAA (Research in Astronomy and Astrophysics), 18, 009
Zhu, C., Lü, G., & Wang, Z. 2015, MNRAS, 454, 1725
Zou, Z., Zhou, X., & Huang, Y. 2020, RAA (Research in Astronomy and Astrophysics), 20, 137